technical memorandum Daresbury Laboratory

DL/SCI/TM52A

SRS CAVITY MICROWAVE WINDOW FAILURE INVESTIGATION:
THEORETICAL AND EXPERIMENTAL FIELD ANALYSIS

by

R.A. RIMMER, SERC Daresbury Laboratory

JANUARY, 1987

Science & Engineering Research Council

Daresbury Laboratory

Daresbury, Warrington WA4 4AD

ISSN 0144-5677

SRS CAVITY MICROWAVE WINDOW FAILURE INVESTIGATION: THEORETICAL AND EXPERIMENTAL FIELD ANALYSIS

R.A. RIMMER

Abstract

This report follows on from the preliminary problem analysis and literature review, and summarises the author's investigations during the second six months of study. A summary of techniques available for analysis of the r.f. field patterns within the SRS cavity window aperture is presented, along with a review of existing computer programs, and an experiment is described which was performed to map the r.f. field patterns using a perturbation method. The success of these investigations is discussed and an outline of further studies is proposed.

SCIENCE AND ENGINEERING RESEARCH COUNCIL
DARESBURY LABORATORY
OCTOBER 1986

CONTENTS

INTRODUCTION

This report follows on from the previous "preliminary problem analysis and literature review"[1] and details two areas of further investigation that have been explored in the first year of the study.

The requirement to analyse the r.f. field patterns in the SRS cavity window aperture is central to the investigation from the viewpoints of estimating power losses in the window (ohmic and dielectric loss), and modelling or understanding secondary electron effects, ion behaviour, sparking, multipactor etc. A two-pronged attack was therefore undertaken, on theoretical and experimental flanks.

The aim of the theoretical investigation was to evaluate methods of field mapping by which the window aperture could be analysed, preferably of a form adaptable or already adapted to computer assistance for accuracy, speed and usefulness of results (e.g. files full of field values could form the input to thermal or particle tracking simulations). Then it was hoped to acquire or develop a code or method at Daresbury for use in the investigation in its own right and as a check against any experimental results that might be obtained.

The experimental approach was directed towards mapping the fields by perturbation or thermal techniques, the former expanding some preliminary work already attempted at the lab, the latter involving development of new methods for looking at the temperature patterns of the window or other parts of the system. It transpired that thermal imaging equipment was not available at this etage of the investigations but it is hoped to include these studies in the future. However, a systematic investigation by perturbation techniques was undertaken, the preliminary results of which are presented here. Complete analysis of the results will be published at a later date and will probably form the basis of a paper submitted to the Particle Accelerator Conference in 1987 in Washington. (It is also hoped to contribute to a general paper on development of the SRS r.f. system at the same Conference.)

1. FIELD ANALYSIS METHODS FOR R.F. AND MICROWAVE ELECTROMAGNETICS PROBLEMS

1.1 General

It is often desired to obtain information about the electric and magnetic fields and resonant properties of a structure or cavity which is to be used in an r.f. or microwave system, e.g. to estimate power losses, reflections impedances etc. Traditionally this was done either analytically, when the geometry of the problem was simple enough for a direct solution of Maxwell's equations, or empirically, by building models and, for static problems, field mapping using resistive paper, electrolytic tanks etc., all of which are time-consuming, restrictive, and expensive.

More complicated situations can be tackled using hybrid analytical/numerical techniquee, such as creating series of higher order modes (or spatial functions) which satisfy the boundary conditions of the particular problem (e.g. a waveguide discontinuity), but this approach (so-called "mode matching", see section 1.2) is still limited to geometries where modes can be described by simple analytical functions such as sinusoids, Bessel functions etc. Truly arbitrary shapee with no obvious analytical solutions can be approached by fully numerical techniques, usually involving a high degree of computer assistance. Such methods include finite difference approximations based on a mesh of nodes in the enclosed space (e.g., cavity in 3-D or waveguide in 2-D), finite element methods (and boundary alsment msthods) which divide the space (or surface) into small elements of known properties, and the Transmission Line Matrix (TLM) method in which the system is modelled by an array of transmission lines with shunt and series stubs such that the voltage on the TLM is equivalent to the frse space E field and so on. There are numsrous other methods available which are particularly suited to special types of problems but lack any real universal applicability.

Wexler[2] compares the relative merits of the principal methods of generating and solving the sets of simultaneous linear equations which describe electromagnetic problems discretised in this manner. He describes direct solution (e.g. by Gaussian elimination), and solution by iterative methods (e.g. successive over-relaxation) and describes the formulation of the matrix eigenvalue problem in which the eigenvalues correspond to frequency domain solutions (e.g. propagating modes or resonant frequencies) and the eigenvec-

tors represent the corresponding E or H field vectors. In 1969 he speculated that future development would be in the field of better, more efficient, numerical techniques and the increasing use of analog computers to speed processing time. In fact since then the major impact on problem solving has been the vast advances made in digital technology while most of the problem solving algorithms have remained essentially close to their early forms. This may be in part due to the desire to keep the methods as general and close to the original physics as possible and partly due to the efficiency of coding that can result from simple program structure. Two decades later the stage is set for a further significant advance with the increasing availability of computers with vector or parallel processing architecture. These are well suited to the solution of matrix or simultaneous equation type problems.

Mittra[3] describes a wide range of techniques, primarily based on mode matching and some variational methods. These are often well suited to problems involving waveguide discontinuities because of the ability to describe series of modes on both sides of the discontinuity (e.g. mode converters) (see section 1.2).

Davies[4] describes and compares several techniques for approaching the problem of solving hollow waveguides, including finite difference and simple finite element methods, polynomial approximation (where a function is approximated by a truncated series) and point matching which appears to be a kind of transformation using Green's theory to reduce the number of dimensions of the problem (e.g. 3-D volume problem reduces to a 2-D surface problem, akin to the boundary element method).

Tortschanoff[5] also reviews some of the techniques available and programs around in 1984, being primarily concerned however with electro- and magneto-static problems at CERN.

1.2 Mode matching methods

Some problems involving simple discontinuities, such as steps or irises in waveguides etc. lend themselves naturally to mode matching techniques. For example a simple step discontinuity can be analysed by creating a series of ordinary waveguide modes before and after the step, and matching these

functions in the plane of the discontinuity to satisfy the boundary conditions. Usually terms are present in the series solution which correspond to modes which are "cut-off"; these do not propagate but represent local energy storage around the aperture. Some new modes will propagate, a property which leads to the use of such dicontinuities in mode converters.

Wexler[6] describes this process of summing normal modes of propagation using the modal analysis method to study discontinuities and bifurcations of rectangular waveguide and coupling between guides, including higher order mode coupling.

Masterman describes the modal analysis process in detail in his thesis[7] and applies the method to some specific examples. A computer is used to perform the mode matching process but accuracy relies upon careful choices of the types and numbers of modes considered in each region.

Mittra's book[3] outlines a wide variety of methods based on this approach and discusses the relevance of each to particular types of problems, and as such is a useful introductory text.

Simple mode matching techniques cannot however readily cope with double discontinuities which are close enough together such that they cannot be treated individually, although an iterative process can be applied in some cases whereby the first discontinuity is analysed, then the second is done using the incident modes from the first solutions, so that any effect of the second propagating back up the guide is included in a re-analysis of the first and so on. Given the right conditions this may converge on a valid solution. Lee, Jones and Campbell[8] discuss the problems of convergence of iris-type problems and give some general guidelines for efficient numerical computations.

When very thin irises are considered, the number of terms required in any mode matching procedure becomes very large and an approximation must be made by truncating this series at an appropriate point.

Masterman, Clarricoats and Hannaford[9] discuss this problem and derive some numerical results for "infinitesimally thin" irises. Kooi, Leong and

Thng[10] use this method to study the problem of coupling from a circular waveguide to a cylindrical cavity via a circular iris.

Harrington and Mautz[11] take a general approach considering coupling between two arbitrary regions via an arbitrary sized and shaped aperture. They go on to support Bethe's theories of coupling by small holes.

One of the main limitations of the basic method is that it must be possible to express the fields in any regions of the problem as a set of modes or spatial functions. This obviously limits the range of shapes that can be used. Generally speaking, rectangular or circular shapes should present no significant problems, even ellipses could be included, but more complicated geometries are not easily described. This limitation means that the mode matching method cannot be directly applied to the SRS waveguide/cavity transitions because although the waveguide and aperture could probably be described by mode series, there are no such analytical functions which correspond to the cavity modes. A rough approximation could be made by modelling a system coupling into a pill-box or elliptical resonator but this could only be of limited use probably not justifying the difficulty of formulating the problem. The picture is further confused by the dielectric discontinuity in the coupling aperture caused by the alumina window which makes for a complicated set of matching conditions at the four boundaries, and the fact that any junction between a circular pipe and a cylindrical or elliptic cavity through the curved wall section will not lie in one plane but will have a complicated shape.

Zhu and Wu[52] use a simple version of the mode matching approach with good results by careful choice of the regions and boundaries within the problem of a re-entrant klystron cavity (see other methods, section 1.6).

1.3 Finite difference method

Finite difference methods for approximating continuous functions have been in use for very many years, based on the discretisation of the function into a set of points at which the value of the functions is known or is to be calculated. Most engineering-oriented mathematics texts provide a general explanation of the method. For electromagnetic field problems the functions are generally second order partial differential equations such as the

Laplace, Poisson (static) or wave equation (high frequency) developed from Maxwell's equations within some system of boundary constraints, e.g. waveguide walls. Applying finite difference methods to the solution of such functions in two or three dimensions (e.g. for the electric field strength in a waveguide or cavity) generates a large number of simultaneous equations. This process is often performed by dividing up the regions into a regular grid and at each point or "node" on the grid writing a finite difference approximation equation which links the field value at that point to the values of its nearest neighbours. Nodes on or adjacent to conducting boundaries or special boundaries such as dielectric surfaces or symmetry planes (which form a logical boundary for the model) require different relations to those within the bulk of the area or volume. When relations at all the points have been formulated the simultaneous equations so produced have to be solved. For small systems these can be solved directly, e.g. by Gaussian elimination (noting the limitations of that method and employing pivoting etc. to minimise numerical errors). For larger sets this is impractical so iterative methods must be used to converge on a solution (this is where differences in algorithms etc. can improve speed and accuracy). The basic method relies on being able to make a good guess at the starting values at every point to ensure rapid convergence to a real solution. On each iteration the values are corrected according to the values of the surrounding points using the appropriate finite difference equations, a method called relaxation. Convergence may be speeded up by over-correcting by a factor, usually < 2, known as Successive Over-Relaxation (SOR). In reality there is often more than one possible solution (e.g. modes in waveguide) so the system corresponds to a Matrix Eigenvalue Problem. Using various clever matrix manipulation techniques it is possible to produce a set of eigenvalues which correspond to these solutions, although these methods sometimes throw up spurious eigenvalues (solutions) which do not correspond to a real physical solution, thus care is needed. Most modern programs based on this method will produce a set of eigenvalue solutions up to a certain user-requested level, e.g. the lowest n modes of an r.f. cavity, but the higher the order of the modes the longer is the computation time required. Successful modern computer codes usually employ algorithms or checking routines that minimise the production of non-physical solutions or detect and reject them to improve reliability of the results.

Wexler[2] describes the finite difference method, and methods for solving the syetems of equations, in some detail and is a good introduction to the subject although some of the ideas about adaption to computing are extremely dated.

Perrone[12] givee a fairly simple explanation of the principles using one-dimensional examples (such as stretched strings) and compares the method with simple finite element analysis.

There are variations on the basic method which increase the accuracy or make the method easier to apply, such as taking a larger number of adjacent nodes lnto account in the difference equation, or using higher order polynomials to fit between the points to minimise errors, ae described by Jain and Holla[13]. Lau[14] deecribes a method for using curvilinear discretisation of the space so that a complicated geometry can be made to produce a simpler set of equations, by transforming from a global (real) to a local (mesh) coordinate system. He uses the example of evaluating the torsion in a triangular bar. Another way to increase accuracy is to perform a sort of iterative procese whereby the first solution is used to refine the shape of the mesh for successive runs and so on, e.g. cramming the mesh where there is a high density of field lines.

Edwards[15] describes one of the first uses of the method for the calculation of resonant frequencies of an r.f. cavity (for a proton linear accelerator) and one of the earliest computer programs in the field, just pre-dating the work of Taylor and Kitching[16] at Harwell on the same aort of problem. Ths cavities had rotational symmetry so the problem, expressed in cylindrical coordinates with no azimuthal variations, became two-dimensional. All of the early codes exploited this method to make the meshes required of a reasonable size for the computers of the time.

Albani and Bernardi[17] were the first to describe a code based on a truly three-dimensional model allowing arbltrary shapes, including blocks of dielectric material placed anywhere in the model. The jump to three dimensions, though conceptually reasonably easy had to wait for the technology of computers to progress to the stage where 3-D meshes could be supported.

Weiland[18,19] describes the process of solving Maxwell's equations in three dimensions and describes the sort of methods that have gone into his codes which are amongst the most advanced of their type at present.

The move to three dimensions highlights another problem of this sort of modelling and that is the task of preparing the model and analysing the data. This was possible in two dimensions with relatively simple pre- and post-processors but 3-D models require much more flexible and powerful processors to cope and this is as important as good numerical results in the building of a workable system for engineering simulations and CAD purposes.

The finite difference method like other types is ideally formulated to take advantage of the imminent availability of powerfui parallel processing or "vector architecture" machines. Versions of many codes already exist for machines such as CRAY and CYBER parallel processors but these are currently too expensive for most applications.

1.4 Finite element method

The finite element method was originally developed with a bias towards mechanical and structural problems where the system under investigation contained too many structural elements or degrees of freedom for conventional analysis to be practical. The properties of individual elements such as beams are modelled in local coordinates (i.e. a coordinate system which makes most sense for the element taken in isolation), and a full model constructed in global coordinates made up from a small number of different types of elements. Where elements join a numbered node is defined and for each element a relationship is known between all ths numbered nodes, e.g.between the force and displacement at each end of a beam and the stored energy within the beam element. Boundary conditions are imposed by fixing nodes or constraining them to move in certain ways, e.g. removing one or more degrees of freedom, and a stimulus is defined by applying known forces to other nodes, e.g. wind loading on one side of a building or sideways forces on the base nodes of a structure to simulate an earthquake. An iterative process is then applied, ln a similar way to the relaxation of a set of simultaneous equations generated by a finite difference model, until a solution for the set of node displacements and forces (and element stored energies if needed) is obtained. The stimulus can be static, like e.g. the water pressure on a dam, leading to

eteady state deformation of the model, or dynamic, iike the shaking of the ground in an earthquake, the latter input causing either a time history output of the structural deformation or a frequency spectral analysis of the resonant frequencies of the structure, depending on the type of simulation being run. Like a finite difference model, a finite element modei may have more than one soiution, in fact wlth complicated etructures this is very likeiy, and the model can once again be formulated as a matrix eigenvaiue problem, where in the earthquake example above the eigenvalues repreeent mechanical resonances of the structure (the eigenvectors representing forces, displacements or accelerations depending on the model). Non-phyeical solutions can be a problem with this method too.

Sheffler[20] and Zienkiewicz[21] both provide good general introductions to the method and its traditional applications; Zienkiewicz is probably the most referenced text in the literature in this field and is probably a good working guide for anyone entering into the eubject, but is limited to traditional applications of etructural or thermal or continua problems.

Modelling of continua euch ae heat or fluid flow problems or plastic deformation of solids (and even etructures in failure) ls another area where this method is powerful. Thie type of analysis has strong parallels with the type of models needed for electromagnetic problems and in recent years interest has increased in the use of finite element analysis in this way. Taking the eimple example of the heat flow model, the elements are eimply small regions of the whole volume over which the temperature (or pressure in the fluid flow caee) ie assumed conetant. The heat (or fluid) flow between one element and the next is eimply a function of the temperature (or pressure) difference between the two and the conductivity of the boundary. The heat content and the temperature of the element are eimply linked by the heat capacity of the element. Boundary conditione are imposed by defining surfacee of conetant temperature or conceivably constant heat flow and a finite element analyeie would yield etable temperature distributions. There are direct analogies in the field of electro- and magneto-statica where, for example, surfaces of constant voltage would induce etable field patterns within the model space. For an alternating stimulus (or boundary condition) the model again becomes an eigenvalue problem and could yield resonant modes of structuree, for example. Much interest has been generated by the use of

low frequency stimuli to look at the generation of eddy currents in conductors in electrical machines, etc.

Mathew and Brody[22,23] employ a 3-D heat transfer model by finite eiements to determine the temperature distribution in a continuous casting process and from that deduce the inherent thermal stresses generated.

Armor and Chari[24] describe a similar 3-D thermal simulation to study heat flow in the stator core of a turbine generator, discussing choice of eiements and eolution algorithm. Their results agree well with experimental data.

Chari et al[25] combine electromagnetic and thermal analysis (in 2-D) to try and build a unified model of electromagnetic heating in a conductor. They also describe operations of the GE2D finite element software package and its pre- and post-processors.

Konrad[26] presents a good historical review of the development of finite element analysis in electromagnetic design, concentrating on electrical machines but mentioning also solution of axisymmetric r.f./microwave cavities. He discusses the use of CAD packages and gives examples of some of the impressive results that can be achieved by electro/magnetostatic modellers. The paper is also a good source of references for anyone further interested in the field.

Simkin and Trowbridge[27] describe a system for elecromagnetics CAD using a dedicated machine of modest capability and describe the procees of mesh generation and post-processing with intereeting graphics software.

Lowther[28] describes attempts to build a 2-D finite element package on a microprocessor. This is obviously a fairly limited facility at present though personal computing power is steadily becoming cheaper and more available.

Finite element models can have trouble when eystems have open boundaries, e.g. conductors or air spaces running off to infinity. A simple approximation is just to extend the mesh to a distance significantly far from the

important part of the model as in McAulay's 2-D model of a dielectric loaded railway line[29]. The problem is similar to contemplating the effect of the boundaries of an electrolytic tank in an empirical solution of a static field problem. If the tank is large enough they can be ignored, if not it is sometimes possible to shape the tank so that it fits the equipotentials of the first solution such that successive attempts should be influenced less by its presence. Silvester et al[30] describe a method where a very large annulus around the open boundary problem can be modelled but where the external elements are manipulated to form a matrix which only includes nodes on the inner boundary (e.g. edge of conductor) which means the model is only as big as the inner region when it comes to the actual numerical processing. They present examples in 2-D of external fields around conductors, charged strips, irregularly shaped busbars and parallel plate capacitors.

Babuska and Rheinboldt[31] address the problem of assessing the reliability of results, rates of convergence etc. A crude method of determining the validity of a solution is to refine the model using a smaller mesh and see if the results change. (This applies to virtually any numerical method.) However this does not show up the possibility of a non-physical mode.

Solutions of systems at high frequencies started with attempts to model waveguide problems (essentially 2-D) with odd shapes or inhomogeneous loading of dielectrics e.g. Csendes[32], who studied various configurations of dielectric blocks in rectangular waveguides. He also describes a similar problem solved by mode matching techniques.

Konrad[34,35] describes solutions of axisymmetric structures (linac cavities) by the finite element method, having advantages of computer store and run time over traditional finite difference methods. Recently[36] he describes proposals for new "variational finite element" approach for three-dimensional cavity problems, using a "versatile curvilinear subparametric brick-shape element with 27 interpolation nodes". Advantages claimed are more direct solutions and fewer (or zero) spurious non-physical modes.

Webb et al[37] and Ferrari[38] present a general approach to the development of a three-dimensional finite element structure for high frequency investigation of arbitrary shaped closed systems containing losey inhomogeneous materials, but the method does not appear to have been developed to the extent of others or to the point of a usable computer code.

Hara et al[39] describe a working 3-D code but this too is of limited capability (they present examples of smoothly deformed rectangular and cylindrical cavities) but the program MAX3D does include all the essential ingredients of a workable system with pre- and post-processors to complement the solver. In the same journal Bryant and Freeman[40] describe a highly interactive three-dimensional mesh generator (pre-processor) capable of use on a modest computer allowing the engineer the facility to build models interactively on a local machine before submitting a job for numerical processing elsewhere. These two examples must point the way for future developments.

Finite element analysis in the field of microwave/r.f. analysis and modelling is still lagging behind developments in the structural/mechanical/civil engineering disciplines, and also behind comparable solvers based on finite difference and other techniques. At the time of writing the author is not aware of any finite element based CAD system which could be used to model a system as geometrically complex as the SRS waveguide cavity transition. Development of such a system in the future could have distinct advantages in the possibility of linking the electromagnetic modeller with thermal and hence mechanical (stress) modellers. This would allow, for example, the fields in a dielectric window to be analysed, generating a heating profile (by dielectric loss), and hence temperature and stress profiles.

This would solve a large part of the problem faced by the author but is still a long way off so separate existing methods must be employed as well as possible to achieve the same result.

1.5 Transmission Line Matrix (TLM) method

The TLM method approaches the solutions of electromagnetic fields in a slightly different way to finite difference or finite element techniques (although mathematically it can be shown to be equivalent to a special case of the finite difference method) in that it models the behaviour of the inside of a cavity or system with a mesh (or equivalent circuit) of interconnected transmission lines. It can be shown that there is a direct analogy between parameters on the equivalent circuit and free space, e.g. between the

transmission line voltage and the E field in space. In fact an equivalent set of rules to Maxwell's laws apply so the mesh is a direct model of real behaviour. The method has general advantages over other techniques which may make it a promising method in the future. The limitations of the model appear only in the accuracy of modelling the geometry, unlike other methods, since an exact solution can be obtained for the transmission line matrix (subject to sufficient numbers of iterations).

The method is inherently suited to including dielectrics etc. or lossy materials simply by the addition of parallel stubs at the nodes (which are where the transmission lines join). It is also possible to model boundaries which do not correspond to regular mesh points by joining shorter lengths of line from the nearest mesh point to the boundary and suitably terminating them. This development significantly improves the modelling ability of the system.

The principal method of solving a problem is in the time domain and this can be used in two ways, either a time history can be studied of the field at any node or nodes, after a known excitation, or a shock excitation is applied to the model (so as to couple to all possible modes) and the time history is subjected to a fast Fourier transform, which highlights the resonances as peaks in the frequency domain.

The method could be adapted to include charged particles, e.g. for the excitation of a cavity by a bunch of electrons. It was even suggested to the author in a discussion with Professor Johns, who is chiefly responsible for the development of the method, that the process might be able to model the production of synchrotron radiation by the acceleration of electrons.

The method was first developed in two dimensions and applied to waveguide problems as by Johns[41] who discusses the application of the method and the errors likely to arise in practice. Advantages are described in execution time and storage on a computer compared to finite element analysis of comparable accuracy.

The method was subsequently expanded to three dimensions (four including time) as described by Akhtarzad and Johns[42,43], giving results for simple

rectangular cavities with dielectric blocks. The same authors describe applying the process to modelling microstrip resonators[44], and results including dispersion characteristics, discontinuities and investigation of a low-loss mode.

Further developments include the use of models with irregular internodal spacing[45] and development of a new type of node, the so-called "condensed node", described by Johns[46] in a recent paper which is also a useful resumé of the method in its current state of development.

The TLM method is a powerful and quite well-developed process which has been incorporated into computer codes (see section 1.7) which demonstrate its potential but fall short of a CAD capability. However a link has been established by creation of an interface between a TLM solver and the commercial DOGS graphics/drawing package. This allows existing software and hardware to be incorporated into a CAD system which may prove to be another pointer to future developments. The TLM package currently available to universities and SERC users, however, has no such sophisticated pre- and post-processing capability and is not the most attractive proposition for modelling the SRS waveguide/cavity transition, although with time and patience it might be possible.

Levy[47] describes a network analog method for solving static problems which is similar in concept to (though simpler than) the TLM method, consisting of a resistive mesh or net and is non-iterative, and shows how the method can make fitting of boundary conditions relatively straightforward. For static problems it is quicker than, say the finite difference method, because it is solved directly and is also less error prone.

1.6 Other methods

Some methods exist which have applications in a few specialised problem areas but lack widespread usefulness and therefore have not had the development of, say, finite elements, like the Monte Carlo random walk method[48] which can be a quick and easy method of solving some types of static field problem. Others, like variational methods, can be used per se or incorporated as part of other techniques. In general, variational procedures involve iterations directed to minimise a variable which usually represents the stored energy of the system. A minimum energy solution usually corresponds

to a stable physical state. English and Young[49] describe a variational approach to formulating Maxwell's equations in cylindrical waveguide problems. Spielman and Harrington[50] include a variational step in their eigenvalue solution for waveguides. Konrad[51] also describes a vector variational formulation for field problems, containing an appraisal of other variational methods applications not included here. This method is generally applicable, he claims, and the derived functional is suitable for solutions by discretisation by finite difference or finite element methods, but gives only the frequency solutions, not the field patterns.

The boundary element method, as expounded by Mercy[52] is similar to the finite element method but has the distinct advantage of only needing a description and meshing of the surface of a model to perform a 3-D solution. This method is particularly useful where the model is not a closed system, e.g. with stray fringing fields going off to infinity. Although the technique is only recently attracting attention for CAD purposes (chiefly still for electrostatic problems) its inherent advantages may make it an important contender in the future.

Zhu and Wu[53] describe the solution of re-entrant klystron cavity by splitting the geometry up into concentric cylinders (a solid cylinder through the beam holes, a small hollow cylinder for the space between the drift tube faces, and a large hollow cylinder for the bulk of the cavity) of known solution and matching series of modes at the boundaries. They report good agreement between computed and experimental results with a simple program and small core-storage requirements. This example shows how for a specific case one type of method can have an edge over generalised multi-purpose methods. If as in the above case the program is only required to handle cavities which are variations on the same geometrical theme, then generality to all types of cavity is useless and even detrimental if it hampers the effectiveness of the specific requirements.

Not only may the solution suffer from the generality of the method employed but, for example, a complex pre-processor required for general problems may be <u>less</u> efficient for simple cases if, say, the cavity can be uniquely defined by a handful of parameters which could be entered into the program in one data statement. Of course this is not usually the case and in

development of a new method or program one strives for generality to appeal to the widest possible number of applications (especially if the result is to be a commercial package).

1.7 Existing programs for electromagnetic problems

At present there are a number of programs and packages around, of varying degrees of sophistication. Some have been in use for many years and have proved their worth by their longevity, some represent developments of earlier programs and some are very new, repreeenting the state of the art in terms of algorithms, computer hardware capability and graphics. Obviously there are new codes being developed all the time so this review is meant to be a brief outline of the present leading "market contenders" known to the author. Availability of these codes is difficult to assess; some are in general circulation, while others are subject to stringent commercial restraints on their supply and use.

The aim of most packages and programs is broadly a three-stage process, first to prepare a model of the structure or cavity, secondly to solve for the fields either in time or frequency domains (or both), and thirdly to present the results in a meaningful way. If any one of these stages is neglected then it does not matter how good the others are, the package will be difficult to use. It is noticeable that modern programs are generally more "user friendly" in this respect. Ideally the system should be usable by anyone who knows about the model geometry and can recognise the results required but who does not know (or want to know) about the intricacies of the numerical processes involved, other than for the program to give him/her some estimate of the reliability of the result.

The history of the development of such r.f./microwave packages, neatly summarised by Weiland[54], started with the desire to design particle accelerator cavities using a computer program, essentially a two-dimensional problem as they had rotational symmetry. Developments to include higher order modes and modes with azimuthal components followed until the development of programs for three-dimensional structures of arbitrary shape, necessitating very large meshes and hence big computers and long runs. Coupled with this, as described above, were developments in input and output techniques.

The first reference to the use of computer programs for the solution of cavity problems known to the author is by Edwards[15] called MESSYMESH closely followed by Taylor and Kitching[16]. These early attempts were crude but effective and within a few years the first real package in the field was described[56]. This program LALA was the first design package and was the seed of many others, indeed variants are still in use today for design of rotationally symmetrical cavity resonators, and it has spread to many countries and institutions throughout the world.

, LALA is a simple finite difference solver that works on a regular two-dimensional mesh (r,z in cylindrical coordinates), with the cavity boundary approximated by a zig-zag boundary of the nearest mesh points. Only one quarter of the cavity need be described, the rest is implied by symmetry. Input to the program is relatively straightforward, as a series of coordinate points, mesh interval, some application specific variables, an initial guess for the frequency and field distributions (some variants do this automatically assuming a certain mode type by filling with a Bessel function or other simple approximation). Output is in the form of frequency, field distributions, cavity parameters (Q, impedance, stored energy, etc.) and plots of electric field lines, axial electric field strength and electric field strength around the metal boundary. The program works well, within its limitations, and is sometimes used to get a rough estimate of cavity parameters before running another longer cavity simulation program.

Rich and MacRoberts[57] describe a development of LALA which includes the magnetic field distribution and more sophisticated handling of the boundary, both in the input and in the numerical process.

It was not until the 'seventies that a successor came into widespread use in the form of SUPERFISH[58]. This and its later development ULTRAFISH[59] are much more sophisticated. They employ matrix techniques to find all the modes using an eigenvalue formulation. This is a significant advantage over LALA which required a good guess at the new frequency and fields to find other modes.

The latest development of LALA known to the author is by Fernandes and Parodi[60], called LALAGE. This extends it to include higher order modes and

multicell structures, keeping the efficiency of the successive over-relaxation (SOR) method used in LALA. This requires less memory than SUPERFISH etc.

ULTRAFISH and a few others have the capability of finding modes that are not cylindrically symmetrical (within the cylindrically symmetric structure), and have azimuthal (or θ) dependence. These modes can be a problem, e.g. in accelerators where particle beams may not be quite axial for some reason.

1983 saw the appearance of URMEL[61], also finite differance based but with a well-developed matrix solver based on a square mesh that can be subdivided into triangles if needed. URMEL finds all modes in ascending frequency from the fundamental and gives graphical plots of field patterns as well as numerical data, if required. A further development to use a fully triangular mesh and allow dielectric or permeable inserts, called URMEL-T, has since been released to expand on this reliable base.

Developments in the finite elements field have dragged well behind the finite difference codes described above. However progress has been made in the electro-/magneto-static case, typified by the TOSCA program described by Simkin and Trowbridge[62]. TOSCA is a truly three-dimensional modeller and may include dielectric and permeable materials. Of necessity it has a fairly comprehensive pre- and post-processor to aid modelling and analysis of results. It is also possible to define regions of uniform potential and include solenoids, coils and permanent magnets; these facets betray its intended role which is the design of magnets and electromagnetic assemblies for the accelerator world, at which it excels. It is of course of little practical use for the SRS window investigation but warrants a mention here in this general appraisal for being a typical state-of-the-art finite element code. The author is not aware of any 3-D electromagnetic high frequency solvers based on this method in general use at this time, despite some exploratory work in the field[34-38]. There is a code called MAX-3D[39] which fulfils the basic specification of pre- and post-processors with a finite element 3-D solver in between (the pre-processor even contains an automatic mesh generator) but it can only handle rectangular or cylindrical cavities or those with "smoothly deformed parts". It does however use an eigenvalue method, so producing a frequency domain (spectral) output.

Meanwhile, a parallel development by Professor Johns and the Nottingham University group produced the first available code based on the TLM method, called TLMRES[63]. This is an impressively compact FORTRAN code requiring little memory even when running, but the trade-off is a rather crude form of input and output. The user is left to design a square mesh of nodes based on the model geometry and enter these as a set of coordinates (particularly tedious for a large 3-D problem) and then to decide how and where to excite the mesh. The program then proceeds to produce a time history of the field at a given point, in the form of numerical output which is taken by the output routine and turned into a frequency domain (spectral) plot by a fast Fourier transformation. In this form the program is widely available, e.g. through university channels but does not seem to have made a great impact. An important development in the CAD field, however, is the release of an interface between the TLM solver in its most advanced form (condensed node version) and the widely used DOGS drawing office system[64]. Thus any institution that has DOGS can buy the interface and solver and have a ready-made CAD package of modest capability. It should be able to model quite complicated 3-D systems and may be of use, for example in microwave tube design where it could ease "cold test" dependence on building dummy slow wave structures, cavities etc. and measuring their properties.

The 1980s have also seen the rise of the finite difference based fully 3-D codes. Wilhelm[65] describes the extension of his two-dimensional code CAVIT into three-dimensional CAV3D, and describes the problems encountered in accurately meeting a complex 3-D boundary. Input and output are not well developed in this code, however.

The two most recent and most well-developed 3-D codes in the market place are SOS[66,67] from Mission Research Corporation in America and MAFIA[54,55,68] from DESY in West Germany, the latter only just released late in 1985, (in fact the post-processor is still being written and developed at the time of writing).

SOS (the name comes from Self-Optimised Sector, which describes how the program organises itself on machines with limited core memory) was developed originally for plasma-physics type simulations and is currently available for CRAY and VAX 11/780 (the latter rather slower but not everyone has a CRAY at their disposal). Availability outside the USA is unknown at present, at the time of writing there are no users of the code in the UK and being a high-tech. product it probably falls under the USA's strict export of technology restrictions. It uses a finite difference type method, accounting for the presence of currents and free charges by the Particle In Cell (PIC) method (also used by an earlier plasma physics program EMPIRE[69] used on the SERC CRAY computer which used to be at Daresbury Laboratory). It includes dielectric and permeable materials and any geometry entered by the user via a versatile but not particularly sophisticated or user friendly pre-processor. The model is excited as defined by the user, either shock excited or driven at a set frequency, and solution is as a time history of field parameters at user selected points. The user need then only perform a Fourier transform to get the spectral response, showing all the modes so long as the excitation is arranged to couple to them all (just as a cold test of a microwave structure will not reveal all the modes if not driven appropriately). The limit to the resolution of the modes that can be found is the length of the time step in the simulation. Work is currently underway in the USA to incorporate SOS as part of a microwave tube maker's CAD package, which would give a tube manufacturer a distinct advantage in the time taken to design a new tube.

MAFIA (MAxwell's equations by Finite Integration theory and their Application), developed at DESY by Weiland and his group, is a suite of programs* for analysing three-dimensional structures and cavities, principally aimed at the particle accelerator field, but having a broader range of applications than that by virtue of the flexibility of the modelling and solving routines. The problem is described by modelling the geometry in 3-D using a highly interactive graphical drawing package, on a colour terminal, which includes an automatic mesh generator to fill the space inside the system. There are then two methods of analysis available, the first being a complete modal analysis[70] of the structure finding all modes up to a specified order or frequency (N.B. the algorithm is such that non-physical solutions or "ghost modes" are eliminated and cannot appear), the field distributions, resonant frequencies etc. of these modes can then be output using the post-processor graphics package (when this is released). Alternatively, and of more inter-

*A development from URMEL and URMELT into three dimensions

est to accelerator physicists, the model can be excited by simulating bunches of electrons shooting down the axis of cavities at practically the speed of light[71] and the output is in the form of a time history of the "wake fields" induced in the structure or a frequency domain spectrum of modes excited. MAFIA is available from DESY to all universities, laboratories, or non-profit making organisations which have an exchange agreement, or may be used commercially by special agreement negotiated with DESY. Versions exist for IBM, CDC, CRAY and VAX computers.

Because of the availability and sophistication of this package it has been obtained by the author, through the exchange agreement between Daresbury Laboratory and DESY, for application to the SRS waveguide/cavity window problem and is currently being installed on the Daresbury NAS 7000 computer for evaluation and testing. This is not a straightforward procedure as the Laboratory does not support any of the graphics language options (PLOT10, DISSPLA, or GKS) so the plot software is being converted to GHOST-80 for use at Daresbury.

It is hoped to do a more thorough analysis of the SRS accelerating cavity geometry than has ever been done before, including windows and side-ports and to build a model that extends into the waveguide system through the window aperture to find out what the fields look like and compare them with results from perturbation experiments and thermal studies. Modal studies of the system may also be of use to accelerator physicists studying beam instabilities etc.

2. EXPERIMENTAL INVESTIGATION OF WINDOW FIELDS BY PERTURBATION METHODS

2.1 General

The experiment was designed to extend the work of Dykes and Garvey[72] who drilled small holes in the side of the waveguide such that a dielectric bead could be drawn across a diameter or chord of the window. By perturbation theory (see Appendix 1) this should produce a small shift in the resonant frequency of the cavity/waveguide system, the magnitude of the change being proportional to the square of the electric field strengths. The drawback of this method was the difficulty of inserting or removing the bead (the waveguide system had to be unbolted) to change positions from diameter to chords either side, or to measure the insertion frequency shift from no-bead to with-bead, and consequently the time taken to measure the insertion shift made drift of the cavity properties a major problem.

The author's experiment was designed to allow rapid insertion or removal of the bead of perturbing object and easy relocation of the positioning mechanism between chords on the window surface. It was also made simple to move the positioning mechanism between any of four planes above the window to add a third dimension to the mapping process (these were 10, 15, 20, 25 mm above the base (narrow) wall of the waveguide and the dielectric window surface is recessed a further 10 mm below this, in a flange recessed ~ 4 mm, see fig.1). In its lowest position the bead is flush with the waveguide wall, though still ~ 10 mm above the dielectric. From these four sets of readings it should be possible to extrapolate down to the window surface. In addition to the use of a dielectric (mycalex) bead it was proposed to use a copper bead to couple to both electric and magnetic fields and to use copper and dielectric rods to gain information about the direction of the fields.

2.2 Test cavity modifications and equipment

The flexibility of the method is due to the replacment of a section of the waveguide wall each side of the window by a sliding bar, see fig.2. The bar is able to slide back and forth such that the holes drilled in the centre move along the full width of the window. This necessitates having a slot cut along virtually the whole length of the waveguide/cavity transition, which causes two problems: first, it substantially weakens the transition, (which requires bracing before it can be machined) and secondly a slot would drastically disrupt the currents in the walls. The first problem is a minor one simply requiring careful setting up of the equipment, the second can be overcome by making the slider out of copper and ensuring good electrical contact using "knit-mesh" (see fig.2) and by covering the ends of the slots on the inside of the waveguide with conducting tape which maintains the appearance from inside of a continuous wall but allows passage of the slider behind it. Each slider has four holes in a vertical line in the centre through which is passed the nylon line which supports the beads, see fig.3, or rods, see figs.4, 5, 6. The slides are held in place by clamps done up by hand (fig.7). The nylon line passes out through the holes, over a pulley (mounted using an adjustable structure fabricated from Meccano) and on one side is attached to the slider of a linear potentiometer, for accurate posi-

tional data, on the other to a counterweight, (via another pulley) to keep the line taut, see figs.7, 8. The line is passed twice through the beads and variously through and around the rods to prevent any slippage and to keep the rods in their correct orientation, see fig.9.

The standard test cavity arrangement at Daresbury is driven by a 50 kW transmitter via a high power coaxial feeder. For this experiment this arrangement was replaced by a waveguide to low power coaxial transition and fed at signal generator level from the r.f. test equipment.

The r.f. test equipment consisted of a high resolution frequency synthesieer (including sweep function), a network analyser with choice of polar and phase/gain displays and reflection/tranemission test boxes with harmonic generator. These were used in setting up, as in fig.10, and for the perturbation experiment, as in fig.11. A 20 dB broadband amplifier was placed on the cavity pick-up loop so that the harmonic generator was comparing signals nearer in amplitude, thus reducing noise as viewed on the network analyser. Noise proved to be the limiting factor as far as resolution was concerned, as is to be expected when trying to measure frequency shifts of a few hundreds or even tens of Hz on a 500 MHz signal.

Difficulty was experienced with signal instability and noise with the first signal generator which has since broken down completely and been sent off for servicing. The other generator was better but still fairly noisy on the highest resolution of the network analyser. However the perturbation proved to be large enough in most cases that the noise was tolerable.

A fair amount of time was wasted trying to stabilise the cavity water system which was eventually bled of air but could not be made to control the temperature accurately enough. Being a very high Q cavity its resonant frequency is sensitive to tiny changes in volume or shape caused by temperature fluctuations. The water system controls the temperature to within 1°C, probably as good as ± 0.1°C (although this is hard to judge by the digital meter) but within the dead-band of the control loop the temperature was fluctuating quite rapidly, causing the resonant frequency to drift up and down by up to 1 kHz over a few tens of seconds. This meant that during the time taken to make a measurement, by pulling the bead across the window, the

frequency would drift by a greater amount than the perturbation, clearly making accurate results impossible. This was eventually cured by turning off the temperature controller, though leaving on the circulating pump, and letting the cavity temperature drift up and down with ambient temperature. Although the absolute change was much greater, the rate of change and hence drift of cavity frequency was improved by more than a factor of 10.

It was also demonstrated that turning off pumps, heaters, ion gauges etc. did not affect the signal/noise ratio (SNR) at the pick-up loop but leaning on the cavity drift tube arms perturbed the resonant frequency significantly.

2.3 Setting up procedure

Using the transmission test set up, as in fig.11, with a 50 kHz sweep the generator was tuned to show the cavity resonance with no bead. The phase/gain display clearly shows the resonant peak on the gain setting and the sharp 180° phase shift through resonance. The network analyser shows spikes, like markers in the response which are generated internally (for no apparent reason) and cannot be removed. These are a nuisance so the cavity tuner was used to move the resonant frequency to a "clean" area. It is particularly undesirable to find one of these spikes on the phase response near resonance, which is where the perturbation is observed.

Then, using the reflection test apparatus as in fig.10 and the polar display, the matcher position was set by the following procedure. First the polar display was calibrated by feeding into a short-circuited transition of the same type as that on the test gear (fig.10). The spot on the polar display was adjusted to be right on the edge of the screen grid and the phase adjusted until the spot was on a 90° line ("12,3,6 or 9 o'clock"). The display could then be thought of as a Smith chart with the spot on the infinite VSWR position, see fig.12a. The test signal was then fed into the real system, with a sweep of about 300 kHz through resonance to give most of a circle on the display, see fig.12b. The matcher position was then adjusted so that the circle cut the centre spot (VSWR=1) fig.12c, i.e. giving a perfect match at the resonant frequency. This was then left untouched for the rest of the experiment.

2.4 Measurement of insertion loss and cavity Q

Measurement of insertion loss of the system, i.e. difference between the signal going in and that coming out, was achieved as follows*. The cavity system was bypassed by connecting the test signal direct to the pick-up amplifier (taking care that the signal generator was not set to full power) and the channel gain on the network analyser/harmonic generator was adjusted to bring the top of the resonance peak to the centre of the screen height, noting the reading. The circuit was then broken and the cavity inserted causing the signal to drop down or off the display. More gain was dialled in to bring the wayward trace back to its original position. The differences between the new and old readings was the gain needed to make up for the insertion by the cavity, i.e. the insertion loss. Values noted for this experiment were: 5 dB gain required for the s/c test channel (including the amplifier) and 36 dB gain required with cavity, *i.* insertion loss = 31 dB. The harmonic generator is much better able to cope with signals ~ 30 dB apart than ~ 50 dB as would be the case without the amplifier.

The cavity Q was obtained by measuring the - 3 dB bandwidth and the centre frequency, this gave the loaded Q(Q_L). Theoretical unloaded Q (Q_0) is given by the formula

$Q_0 = (1 + \beta)Q_L$ (where β = coupling factor = 1 for perfect match)

The - 3 dB bandwidth and centre frequency were ascertained as follows. A sweep width was selected which showed the response down to below - 3 dB either side of resonance, which was centred in the screen. The generator was then switched to manual sweep and as soon as the control knob was touched the spot appeared on the screen; turning the knob moved the spot through the sweep range showing the frequency on the LED display. Thus the centre frequency and 3 dB points could be found. Typical values for the SRS cavity were cent. freq. 500.174 MHz, - 3 dB bandwidth of 26.5 kHz, i.e. Q_L = 18874, Q_0 = 37748, at about 20°C. Repetition of these measurements gave an estimate of the accuracy by which the - 3 dB points could be determined (note that in absolute terms they could be determined very accurately but the difference was much less accurate owing to the closeness of the readings).

*System in transmission test mode, sweep through resonance, e.g. 50 kHz.

2.5 Experimental Procedure

The frequency perturbation is too small to be observable on the amplitude display but for small deviations around resonance the phase can be considered to vary linearly with frequency and because it changes so sharply (an advantage of having such a high Q system) it is a sensitive indicator of the perturbation. On the most sensitive setting of the phase display (1°/cm) a perturbation of a few hundred Hz shows up as a movement of the spot by several cm, enough to be significant above the noise. There is a filter on the network analyser which can be used in manual mode (spot as opposed to trace) which reduces the higher frequency noise (which tends to spread the spot out), leaving the low frequency noise, observable as an instability or random bouncing of the spot.

The first thing done when taking a set of measurements with a particular perturbing object was to measure the insertion perturbation, i.e. the difference between no object and the object placed in the waveguide next to the wall. This was done by first centering the resonance on the screen with a sweep of ~ 25 kHz by adjusting the centre frequency of the generator (note: if the cavity response had drifted near to a spike on the display, a tweak of the servo tuner could be used to move to another part of the spectrum. However, this is a very unsubtle way of tuning, and is rather a hit and miss process. Once the tuner starts to move it does so over several kHz at a time so it is not possible to perform fine tuning), then changing to the phase response, which on 1°/cm setting looked like a steep straight line through the middle of the screen. It was checked that the sliders were clamped in place but not overtightened as it is easy to distort the walls of the waveguide in this way. The generator was switched to manual and the spot adjusted to the centre of the screen and frequency noted. (Too coarse a sweep in auto mode could give rise to the spot moving in noticeable jerks.) Then the nylon line, already in at this stage (it having been found to have no significant perturbing effect), was removed from the wiper of the linear potentiometer (being careful not to let go and have it disappear out the other side in pursuit of the counterweight!) and one slider removed to allow threading of the object onto the line. The slider was then replaced and the line tied back to the linear pot and held in place by a small piece of tape. This caused the spot to move if the insertion shift was significant and if so it was returned to the centre by adjusting the sig. gen. frequency and the dif-

ference in frequencies noted. If threading the object was tricky and thus time consuming the procedure could be reversed so that the removal frequency shift was measured, being quicker and therefore less prone to drift of the resonant frequency.

The sign of the frequency shift is also important. In this case when the spot is returned to the centre after insertion the frequency displayed is the new resonant frequency and it is straightforward to see if the shift was upwards (+) or downwards (-).

Taking real measurements was done as follows. The sliders, counterweight pulley and linear potentiometer were positioned each that the holes lined up with the appropriate chord of the window. (It was considered sufficient to take readings at 1 cm intervals from the diameter out to the edges.) A scale was fixed to the waveguide on each side to allow accurate alignment of the holes. The object was threaded on the line which was passed through the appropriate holes and attached to the counterweight on one end and the slider of the pot. on the other. With 9 V across the linear pot. the position of the bead could be correlated with the x-travel of an x-y plotter. The x-channel gain of the plotter was adjusted until the travel of the pen was the same as the movement of the object in the guide. The copper bead required a heavier counterweight to prevent excessive sag in the middle of the travel. The amplitude response, on auto-sweep, was adjusted for resonance in the centre of the screen, the phase response on 1° per div. looking like a steep straight line. Switching to manual the phase spot was centred and if necessary the filter was applied to cut down the high frequency noise. Now drawing the bead across the window the perturbation could be viewed on the screen and using the phase output from the back of the display box the phase shift was plotted on the y-axis of the chart plotter. The channel gain and offset were adjusted to give a reasonable sized graph and the apparatus was ready for a measurement. This involved taking up the slack, if any, in the line by pulling gently on the pot. slider, then, with the pen down, drawing the bead across the window and allowing it to slide back slowly, producing two traces on the paper. The pen was then raised ready to set up for the next measurement. The traces were generally coincident unless there was any drift in cavity parameters with time during the measurement, which showed up as a small y-offset between the start and end points. Usually the time taken

for a set of data was short enough for this not to be a problem.

Owing to the large numbers of plots taken, it was found to be convenient to place them in sets on the graph paper, usually eight or nine could be fitted together, e.g. from the central position to the edge, see fig.13. Groups of data taken on the same scale were calibrated in one go by setting down the pen for a couple of seconds, leaving a mark corresponding to the current frequency (blurred out along the y-axis by noise) then shifting the spot and pen by changing the signal generator frequency and spotting another mark on the graph paper. The frequency separation and the physical displacement serve to calibrate the plots. NB: unlike the insertion loss measurements there is a discrepancy between the sign of the perturbation and the apparent calibration. For example, if an object perturbs the spot down the screen (or + y directions on the plotter) this corresponds to the resonant curve moving left on the screen and decreasing in frequency but to calibrate this change by moving the spot down the screen the signal generator must be increased in frequency so the calibration has the correct magnitude but the wrong sign. This must be borne in mind when interpreting the plots.

The sequence of measurements was usually to set up the scales etc. on the central position then take measurements at 10 mm intervals towards one edge, return to the centre and take plots in the opposite direction. It was sometimes necessary to increase the y-channel gain towards the edges of the window if the perturbations became too small or too large, requiring recalibration of course. The signal generator power output had to be kept constant during a set of readings, otherwise there would be no consistency in E field values produced by each plot. Likewise it was necessary to keep the power level the same between sets of readings, e.g. the 3 orientations of the rods or between dielectric and conducting objects of the same type, as these results were to be used in calculations which assume constant field levels. The best way to achieve this was to set the power level, using the operating range meter on the front of the network analyser, then once set to leave completely alone. Furthermore the generator was left running throughout the experiment, hopefully minimising any possible errors due to stopping and starting.

2.6 Results and Data Analysis

Approximately 280 graphs were taken, covering every object in the lowest hole (nearest the window) with the rods in both orientations, i.e. parallel to and perpendicular to the line, then with the rods vertical suspended below the line in the top hole and full maps of the mycalex and copper beads also in the top hole. Then plots were taken in holes 2 and 3 with both beads, but only for half the window as previous plots were practically symmetrical so time could be saved this way. For each set of plots relevant information such as the resonant frequency, Q, temperature, etc. were also recorded for future use if required.

Only the copper bead and copper rod parallel to the line produced significant insertion perturbations, and these were small, see table 1. A full analysis of results has not been completed at the time of writing but preliminary findings are encouraging. Data analysis was simplified by digitising the plots using a digitising tablet[73] connected to an IBM PC. The software to achieve this was written in BASIC by the author (a listing can be found in appendix II). From the file name given by the user, the program diagnosed the type of object and opened a data file. Names for data files were systematically chosen to allow this (see fig.14) and as each set of data had already been given a letter to identify it, this was incorporated into the systematic name. Sets of data were taken as half maps, from the centre to one edge, for convenience (see fig.15). Digitisation was achieved by tracing the graph with the stylus, the program working out data values at 1 cm intervals. Before a graph could be entered the frequency axis was calibrated and the end points of the curve located. This allowed the program to scale the digitising surface in both axes. Each graph was traced at least three times and the data values averaged to minimise "digitisation error", i.e. errors due to interpretation of the data or hand tremble by the operator. The average data values were stored in disk files, along with the number of traces averaged and an estimate of the digitising error involved. Note this is in addition to any experimental or hardware errors that may have been incurred in producing the plots. Once digitised, the data was in a form where it could be systematically manipulated to yield the field information. The program was written to be able to distinguish between beads and rods and digitise the plots accordingly, the difference being that in the perpendicular

orientations (y,z) the travel of the rod is longer than for the bead (see fig.16), so to get the samples in the same place digitising must start ~ 6 mm in from the ends of the plots.

2.7 Preliminary findings

Fig.17 shows the contours of constant electric field strength. Further analyses of the other data should show directional information. Information about $|E|$ or E^2 could be used to imply heating in the dielectric, clearly with this pattern a "hot-spot" will develop in the centre, consistent with observed thermal runaway failures.

Fig.18 shows a map of $|H|$ over the window. There is fairly uniform coverage of the surface with no obvious zero points. This again is consistent with the magnetic coupling/cavity fringing field model.

3. FURTHER INVESTIGATIONS

There is an immediate requirement to continue analysis of the data from the perturbation experiment, this hopefully forming the basis of a paper to be contributed at the 1987 Particle Accelerator Conference in Washington, USA. Furthermore it is intended to use the field information as the input to a thermal model, based on dielectric heating, to try and simulate window behaviour. In parallel with this it is hoped to take some thermal images of the window under load for direct compariaon. It is also intended to commission the 3-D field modelling package MAFIA and attempt a numerical solution for the window fields, providing a further means of comparison. If time permits it would also be desirable to turn the thermal model into a stress model to study mechanical behaviour of the window under thermal stress.

Later in the second year it is hoped to start studying some secondary electron effects; multipactor, x-ray production etc. If MAFIA is working then field information for the cavity etc. should allow electron trajectory plotting simulations to be performed and if modelling is successful then anti-multipactor methods can be evaluated theoretically. A system is being installed in the SRS to monitor waveguide sparks on or around the windows, using four TV cameras mixed into a single video picture using different

colour channels. This should provide more information about surface charging effects which are thought to be linked to secondary electron effects in the cavity or on the window.

This leaves the final year open to try and tie the various effects studied into a coherent heating/stressing mechanism and to predict the likely failure mode, evalute anti-multipactor methods currently in use and to propose, and if possible test, new methods or modifications which might help. Fig.19 is the latest version of the project plan, outlining the stages described above, but as always is subject to re-organisation depending on equipment availability, success or failure of individual steps, etc.

4. CONCLUSIONS

The work so far has brought about the acquisition of one of the most up-to-date and powerful electromagnetic modelling packages available which, when installed, should prove a great asset to the project and provide the most versatile investigative tool yet for analysing the cavity and window fields. The perturbation experiment has been succeesful in its analysis of the localised window fields and preliminary findings are interesting and encouraging. There is much information still to be obtained from the rest of the data awaiting processing, including details of the vector fields around the window.

Table 1

Table of insertion perturbations

Object	Position	Resonant frequency (Hz)		
		with (±10)	without (±10)	shift (±20)
Copper bead	hole 1, diameter	500319995 975 985 875	500319965 955 945 845	30 20 40 30
				Av 30
	hole 1, edge chord	no measureable shift		-
	hole 4, diameter	955 945 885 825 795	895 905 835 785 735	60 40 50 40 60
				Av 50
	hole 4, edge chord	no measureable shift		-
Mycalex bead	hole 1, diameter	"		-
	hole 1, edge chord	"		-
	hole 4, diameter	"		-
	hole 4, edge chord	"		-
Copper rod	hole 1, X, diameter	"		-
	hole 1, X edge chord	"		-
	hole 4, X, diameter	355 345 335 345 335	275 275 245 265 265	80 70 90 80 70
				Av 78
	hole 4, X, edge chord	no meaeureable shift		-
	hole 1, Y, diameter	"		-
	hole 1, Y, edge chord	"		-
	hole 1, Z, diameter	"		-
	hole 1, Z, edge chord	"		-
Mycalex rod	all orientations	"		-

APPENDIX I - PERTURBATION THEORY

The perturbation theory usually applied to resonant electromagnetic problems is that developed by Slater[74-76]. This is also the approach quoted by Ginzton[77], but nons of these gives a clear derivation in general terms. Waldron[78] gives an excellent derivation of the fundamental perturbation formula and aleo talks about practical problems. He mentions the effect of the shape and orientation of the perturbing object, but only considers the sphere mathematically. Nakamura[79] also derives the fundamental formula but goes on to consider form factors for various shapes of perturbing object, analysing dielectric and metallic ellipsoids including needles and disks. This theory will hopefully allow further analysis of the cavity window field baeed on the information obtained using the dielectric and conducting rods. There are many other works on resonant and non-resonant perturbation techniquee but the results quoted here are either from Waldron or Nakamura.

Equations 17 and 18 are thoee required to interpret the perturbation by dielectric and conducting beads. If the stored energy is kept the same in each case, the electric field deduced from the first set of readinge (dielectric bead) can be used to produce the magnetic field values from the joint electric and magnetic perturbation measurements (conducting bead).

Derivation of the Perturbation Formula (see p76-82, Waldron)

Assume normal cavity resonant modes $E = E_o e^{j\omega t}$, $H = H_o e^{j\omega t}$ (1)

where E_o, H_o are functions of space.

After small perturbation by finite or dielectric $E' = (E_0+E_1)e^{j(\omega+\delta\omega)t}$, $H' = (H_0+H_1)e^{j(\omega+\delta\omega)t}$ (2)

assume that the fields do not change much and the frequency shift is small.

By Maxwell: $\text{Curl } E = \frac{-\partial\beta}{\partial t}$ (3)

and

$$\text{Curl } H = \frac{\partial D}{\partial t} \quad (5)$$

$$\therefore \text{Curl } E_0 = \frac{-\partial B_0}{\partial t} = -j\omega B_0$$

$$\text{and Curi } (E_0+E_1) = -j(\omega+\delta\omega)(B_0+B_1)$$

Subtracting: $\text{Curl } E_1 = -j[\omega B_1+\delta\omega(B_0+B_1)]$ (4)

Similarly $\text{Curi } H_1 = j[\omega D_1+\delta\omega(D_0+D_i)]$ (6)

Forming the scalar product of H_0 with (4) and of E_0 with (6):-

$$E_0 \text{ Curl } H_1 + H_0 \text{ Curl } E_1 = j\omega[E_0 \cdot D_1 - H_0 \cdot B_i] + j\delta\omega[(E_0 \cdot D_0 - H_0 \cdot B_0)+(E_0 \cdot D_1 - H_0 \cdot B_1)] \quad (7)$$

in which $B_0 = \mu_0 H_0$ $D_0 = \varepsilon_0 E_0$

$B_1 = \mu_0 H_1$ $D_i = \varepsilon_0 E_1$ (8)

outside the sample

and $$D_1 = \varepsilon_0[\varepsilon_r(E_0+E_1) - E_0] \quad (9)$$

$$B_1 = \mu_0[\mu_r^*(H_0+H_1) - H_0] \quad (10)$$

inside the material (*see Waldron p.77 for gyromagnetic material).

Now use the vector identity:

$$\text{Div}[(H_0 \times E_1) + (E_0 \times H_1)] \equiv E_1 \cdot \text{Curl } H_0 \; ; \; H_0 \cdot \text{Curl } E_1 + H_1 \cdot \text{Curi } E_0 - E_0 \cdot \text{Curl } H_1$$

which by (3) and (5) may be written:

$$H_0 \cdot \text{Curl } E_1 + E_0 \cdot \text{Curl } H_1 = j\omega(E_1 \cdot D_0 - H_1 \cdot B_0) - \text{Div}[(H_0 \times E_1) + (E_0 \times H_1)] \quad (11)$$

substituting into LHS of (7):

$$j\omega(E_1.D_0 - H_1.\beta_0) - \mathrm{Div}[(H_0\times E_1) + (E_0\times H_1)] = j\omega(E_0.D_1 - H_0.B_1) + j\omega[(E_0.D_0 - H_0.B_0) + (E_0.D_1 - H_0.B_1)] \quad (12)$$

Let V_0 be the volume of the cavity and V_1 the volume of the object (i.e. $V_0 - V_1$ = vol. of cavity not occupied)

Integrate (12) over volume V_0

$$j\omega\iiint_{V_0}(E_1.D_0 - H_1.B_0)dV + \iiint_{V_0}\mathrm{Div}[(H_0\times E_1)+(E_0\times H_1)]dV = j\omega\iiint_{V_0}(E_0D_1 - H_0B_1)dV + j\delta\omega\iiint_{V_0}[(E_0.D_0 - H_0.B_0) + (E_0D_1 - H_0B_1)]dV \quad (13)$$

In the region $V_0 - V_1$ eqns. (8) apply and the contribution from this region to the first integral on the LHS of (13) is identical to the first integral on the RHS. Thus we require only the contributions to these integrals from revions V_1. For the divergence integral we have, by Green's theorem:

$$\iiint_{V_0}\mathrm{Div}(H_0\times E_1 + E_0\times H_1)dv = \iint_{S_0}(H_0\times E_1 + E_0\times H_1).nds$$

where S_0 = surface of cavity, n is unit vector normal to element dS of S_0. To the extent to which the cavity walls may be regarded as perfectly conducting, $H_0\times E_1$ and $E_0\times H_1$ are tangential to the walls and their scalar product with n is zero. So the divergence integral vanishes.

Asauming that $\delta\omega \ll \omega$ we now neglect D_1 and B_1 in comparison with D_0 and B_0 ln the second integral on the RHS of (13) (see p.79 Waldron for justification). This approxlmation becomes more accurate as V_1 decreases. (13) now becomee:-

$$j\omega\iiint_{V_1}(E_1.D_0 - H_1.B_0)dV = j\omega\iiint_{V_1}(E_0.D_1 - H_0.B_1)dV + j\delta\omega\iiint_{V_0}(E_0.D_0 - H_0.B_0)dV$$

$$\text{i.e. } \frac{\delta\omega}{\omega} = \frac{\iiint_{V_1}[(E_1.D_0 - E_0.D_1) - (H_1.B_0 - H_0B_1)]\,dV}{\iiint_{V_0}(E_0.D_0 - H_0.B_0)dV} \quad (14)$$

which is the required formula for the frequency shift.

Now, for a perturbing sphere:

For a sphere of dielectric material immersed in an electric field which in the absence of the sphere is uniform and equal to E

$$E^1 = \frac{3E}{\epsilon_r+2} \quad \text{(see fig.20)} \quad (15)$$

This formula holds for microwave fields as long as the sphere is sufficiently small for ths field to be sensibly uniform over a region large compared to the sphere.

The denominator represents a function proportional to the energy (U) stored in the electric and magnetic fields within the volume, so (14) can be written

$$\frac{\delta\omega}{\omega} = \frac{\iiint_{V_1}(E_1.D_0 - E_0.D_1) - (H_1.B_0 - H_0.B_1)dV}{4U} \quad (16)$$

For a dielectric bead there is no change in H or B $\therefore$ H_1 and B_1 = 0

outside the bead $D_0 = \epsilon_0 E_0$

inside the bead $D_1 = \epsilon_0[\epsilon_r(E_0+E_1) - E_0]$

but by (15) $E_0 + E_1 = \frac{3E_0}{\epsilon_r+2}$

therefore for perturbation by a dielectrlc sphere

$$\frac{\delta\omega}{\omega} = \frac{\iiint_{V_1}E_0^2\left(\frac{1-\epsilon_r}{2+\epsilon_r}\right)\epsilon_0 - E_0\epsilon_0\left[\epsilon_r\frac{3E_0}{\epsilon_r+2} - E_0\right]dV}{4U}$$

$$= \frac{\iiint_{V_1}E_0^2\epsilon_0\left(\frac{1-\epsilon_r}{2+\epsilon_r}\right) - E_0^2\epsilon_0\left(\frac{2\epsilon_r-2}{\epsilon_r+2}\right)dV}{4U}$$

$$= - \frac{\iiint_{V_1} 3E_0^2 \epsilon_0 \left(\frac{\epsilon_r - 1}{\epsilon_r + 2}\right) dV}{4U}$$

for sphere radius r:

$$\frac{\delta\omega}{\omega} = - \frac{\pi r^3 E^2 \epsilon_0 \left(\frac{\epsilon_r - 1}{\epsilon_r + 2}\right)}{U} \qquad (17)$$

Note: perturbation by a dielectric bead leads to a negative perturbation, i.e. a lower resonant frequency.

Similarly for a permeable material which perturbs the magnetic field as well, an analogous equation to (15) exists

(for perm.bead) $$H^1 = \frac{3H_0}{\mu_r + 2}$$

so the second term in the numerator of (16) cannot be ignored. By a similar process of algebraic manipulation it can be shown that

$$\frac{\delta\omega}{\omega} = \frac{\pi r^3}{U} \left(\mu_0 H^2 \left(\frac{\mu_r - 1}{\mu_r + 2}\right) - \epsilon_0 E^2 \left(\frac{\epsilon_r - 1}{\epsilon_r + 2}\right)\right)$$

for a conducting sphere the local fields are perturbed as if by a body with $\epsilon_r = \infty$ and $\mu_r = 0$, so the equation reduces to

$$\frac{\delta\omega}{\omega} = - \frac{\pi r^3}{U} \left(\epsilon_0 E^2 - \frac{1}{2} \mu_0 H^2\right) \qquad (18)$$

Note: perturbation by a conducting bead in a strong magnetic field tends to increase the frequency.

```
      APPENDIX  II
10  REM*************************************************************************
20  REM              BOB'S DIGITISER PROGRAM..."DIGIT.BAS"
30  REM*************************************************************************
40  REM   This program is designed to input data from the cavity window expt.
50  REM in the form of large numbers of graphs of frequency shift against bead
60  REM position,using a digitising tablet (GTCO type7 12"x12") and stylus.
70  REM   Once scaled appropriately the end points of each line are identified
80  REM and the graph is traced with the stylus. The program selects data at
90  REM the relevant points and stores the information in a large array.
100 REM   Sets of data are taken 8 or 9 at a time forming a 'half map' of the
110 REM window from the centre towards either the source or the matcher.
120 REM*************************************************************************
130 REM    Variables used in this program ....
140 REM MAP$ (name of current map) LC (line counter, no cm from window centre)
150 REM XIN,YIN (new coord's) YUP,YLO,FUP,FLO (upper & lower Y & freq to scale)
160 REM X0,Y0 X1,Y1 (line end points) Y$ (answer to error prompt , y/n,old/new)
170 REM O$ (chr in MAP$ for orient'n) OFSET (o/s of X data pts for odd rods cm)
180 REM SCALE (Y axis scale Hz/point) XDIVN (no points between X data points)
190 REM XREF (current X data point)   YREF (lin. interpolated ref. point )
200 REM ERCT (sum of errors of current line) T$,F$ (data format string for o/p)
210 REM*************************************************************************
220 ON ERROR GOTO 2030                  :REM trap disk and i/o errors
230 REM*************************************************************************
240 REM dimension all arrays            array meaning...
250 DIM PERTN(9,21)                     :REM PERTN holds current half map val's
260 DIM NATTS(9)                        :REM NATTS holds no. attempts averaged
270 DIM AVERR(9)                        :REM AVERR holds av of mag of point errs
280 DIM XDATA(21)                       :REM XDATA holds current X sample pts
290 DIM YDATA(21)                       :REM YDATA holds current Y samples
300 REM*************************************************************************
310 REM Set up digitiser ,(reset temp.removed) and set remote mode
320 REM*************************************************************************
330 OPEN"com1:1200,N,8,2" AS £1         :REM 1200 baud,No p'y,8 bits,2 stop bits
340 REM PRINT £1,CHR$(1)+CHR$(82)+CHR$(83) :REM ctrlA,R,S is the ReSet string
350 REM Z$=INPUT$(8,1)                      :REM echo'd command + reset sequence
360 PRINT £1,CHR$(1)+CHR$(82)+CHR$(77) :REM ctrlA,R,M sets Remote Mode
370 Z$=INPUT$(4,1)                      :REM echo'd command
380 REM*************************************************************************
390 REM enter filename,if file already exists load in old data else assume new
400 REM*************************************************************************
410 INPUT " want to see existing disk files? (Y/N)";Y$     :IF Y$="Y" THEN FILES
420 INPUT "type map name";MAP$      :O$=MID$(MAP$,4,1)    :REM get orient'n chr.
430 OFSET=0                             :REM bead or rod parallel to nylon line
440 IF O$="Y" THEN OFSET=.6             :REM rod horiz.90 deg. to nylon line
450 IF O$="Z" THEN OFSET=.6             :REM rod vertical
460 REM check if MAP$ exists,if not attempt to open for i/p will cause ERR=53
470 OPEN MAP$ FOR INPUT AS £2
480 REM if no error then file exists so read in all previous data
490 FOR N=0 TO 9
500 FOR M=0 TO 21
510 INPUT£2,PERTN(N,M)                  :REM input all 22 data points of a line
520 NEXT M
530 INPUT£2,NATTS(N),AVERR(N)           :REM No att's av'd & av error for line N
540 NEXT N
550 CLOSE£2
560 REM Error routine returns to this point if file did not exist
570 INPUT "want to rescale? (Y/N)";Y$   :IF Y$="Y" GOTO 940
580 REM find first empty data line in array (NATTS=0)
```



```
590 FOR N=0 TO 9
600 IF NATTS(N)=0 THEN LC=N :GOTO 640
610 NEXT N
620 LC=0                                :REM some data in all lines,def = centr
630 REM*************************************************************************
640 REM write out current line status etc...
650 REM*************************************************************************
660 PRINT :PRINT "current line is";LC;"cm from window centre"
670 PRINT NATTS(LC);"att's av'd to give this data , av error=";AVERR(LC)
680 PRINT "current freq. scale is";SCALE/.0127;"Hz/cm"
690 PRINT "enter commands from pad menu to continue..."
700 REM*************************************************************************
710 REM control now from pad , look for command input
720 REM*************************************************************************
730 GOSUB 1810                          :REM prompt for coordinate pair
740 IF YIN<2200 GOTO 730                :REM not a command point
750 BEEP                                :REM command received indication
760 IF XIN<300  GOTO 640                :REM start new map
770 IF XIN<600  GOTO 890                :REM start new line
780 IF XIN<900  GOTO 940                :REM (re-)scale y axis
790 IF XIN<1200 GOTO 1050               :REM (re-)draw line & av. all attempts
800 IF XIN<1500 GOTO 1540               :REM show current line data
810 IF XIN<1800 GOTO 1420               :REM save current map
820 IF XIN<2100 GOTO 1630               :REM print current map on line printer
830 PRINT"END" :CLOSE :ON ERROR GOTO 0 :END
840 INPUT "old map saved?  Y/N";Y$ :IF Y$="N" GOTO 690
850 GOTO 410
860 REM*************************************************************************
870 REM start new line , reset line counter LC
880 REM*************************************************************************
890 PRINT :INPUT "enter dist. of new line from centre (cm)";LC
900 GOTO 660                            :REM return to pad menu
910 REM*************************************************************************
920 REM (re-)scale Y (freq) axis
930 REM*************************************************************************
940 PRINT :PRINT "spot lower freq. calibration point"
950 GOSUB 1810 :YLO=YIN :BEEP           :REM spot low  calibration point
960 INPUT "type low cal.freq (Hz)";FLO :REM get low  freq point
970 PRINT "now spot upper freq point"
980 GOSUB 1810 :YUP=YIN :BEEP           :REM spot high calibration point
990 INPUT "type hi  cal.freq (Hz)";FUP :REM get high freq point
1000 SCALE=-(FUP-FLO)/(YUP-YLO)         :REM SCALE = Hz / point , = Hz / 5 thou
1010 GOTO 660                           :REM return to pad menu
1020 REM*************************************************************************
1030 REM (re-)draw line , averaging all existing data if satisfactory
1040 REM*************************************************************************
1050 IF SCALE=0 THEN PRINT "NOT SCALED":GOTO 660  :REM stops useless data entry
1060 PRINT "spot starting point (leftmost point of line)"
1070 GOSUB 1810                         :REM get start coordinates
1080 X0=XIN :Y0=YIN
1090 BEEP :FOR N=1 TO 100 :NEXT N       :REM indicat'n of start pt + pause
1100 PRINT "now spot end point (rightmost point of line)"
1110 GOSUB 1810                         :REM get end coordinates
1120 X1=XIN :Y1=YIN
1130 BEEP :FOR N=1 TO 100 :NEXT N       :REM indicat'n of start pt + pause
1140 PRINT "now trace slowly along line from left to right (beep = data point)"
1150 XDIVN=(X1-X0)/(2*OFSET+21)         :REM XDIVN is sep'n of X data points
1160 ERCT=0                             :REM start a new error count
1170 FOR N=0 TO 21                      :REM 22 data points
```

```
1180 XREF=X0+(OFSET+N)*XDIVN            :REM XREF is sample point in pad coords.
1190 GOSUB 1810                         :REM get coordinate pair
1200 IF XIN<XREF GOTO 1190              :REM not reached data point yet
1210 XDATA(N)=(XIN-X0)*10/XDIVN         :REM XDATA is dist of pt from start (mm)
1220 YREF=Y0+(XIN-X0)*(Y1-Y0)/(X1-X0)   :REM lin interpolation to get YREF
1230 YDATA(N)=(YIN-YREF)*SCALE          :REM YDATA is freq pertn in Hz
1240 IF NATTS(LC)>0 THEN ERCT=ERCT+SQR((YDATA(N)-PERTN(LC,N))^2) :REM av of mag
1250 BEEP                               :REM indication of point accepted
1260 NEXT N
1270 PRINT :PRINT "new vals,av.err=";ERCT/22,"old vals av.err=";AVERR(LC)
1280 FOR N=0 TO 21
1290 PRINT XDATA(N),YDATA(N),PERTN(LC,N):REM XDATA in mm , YDATA in Hz
1300 NEXT N
1310 INPUT "good data values (Y/N)";Y$ :IF Y$="N" GOTO 660       :REM junk data
1320 FOR N=0 TO 21                      :REM update data in PERTN & NATTS arrays
1330 PERTN(LC,N)=(YDATA(N)+NATTS(LC)*PERTN(LC,N))/(NATTS(LC)+1)
1340 NEXT N
1350 M=NATTS(LC)
1360 IF M>0 THEN AVERR(LC)=((M-1)*AVERR(LC)+(ERCT/22))/M
1370 NATTS(LC)=NATTS(LC)+1              :REM increment count of no attempts av'd
1380 GOTO 660                           :REM return to pad menu
1390 REM*************************************************************************
1400 REM save current map on disk
1410 REM*************************************************************************
1420 OPEN MAP$ FOR OUTPUT AS £2
1430 FOR N=0 TO 9                       :REM 10 rows of data
1440 FOR M=0 TO 21                      :REM 22 data points
1450 PRINT £2,PERTN(N,M)                :REM output frequency perturbation
1460 NEXT M
1470 PRINT £2,NATTS(N),AVERR(N)         :REM o/p no. att's av'd & av.error
1480 NEXT N
1490 CLOSE£2                            :REM close o/p file , no longer needed
1500 GOTO 660                           :REM return to pad menu
1510 REM*************************************************************************
1520 REM show current line data
1530 REM*************************************************************************
1540 PRINT
1550 PRINT "cm from start,fr.pert'n,av of ";NATTS(LC);"att's,av.err=";AVERR(LC)
1560 FOR N=0 TO 21
1570 PRINT N,PERTN(LC,N)                :REM list data points
1580 NEXT N :PRINT "enter commands from pad to continue...";
1590 GOTO 730                           :REM return to pad (with min messages)
1600 REM*************************************************************************
1610 REM print current map on line printer
1620 REM*************************************************************************
1630 F$="+£££££"
1640 WIDTH "LPT1:",132
1650 LPRINT "DATA FROM FILE ";MAP$      :REM title printout
1660 LPRINT " y\x "; : T$="£££££"       :REM table heading format
1670 FOR N=0 TO 21 :LPRINT USING T$;N; :NEXT N :LPRINT " cm";
1680 FOR N=0 TO 9                       :REM 10 lines
1690 LPRINT :LPRINT
1700 LPRINT N;"cm";
1710 FOR M=0 TO 21                      :REM 22 data points
1720 LPRINT USING F$;INT(PERTN(N,M));   :REM formatted o/p to get table right
1730 NEXT M
1740 LPRINT " av of ";NATTS(N);"att's"
1750 NEXT N
1760 LPRINT :LPRINT
1770 GOTO 660
```



```
1780 REM*************************************************************************
1790 REM subroutine returns coordinate pair in XIN,YIN (pen status byte A$)
1800 REM*************************************************************************
1810 PRINT£1,CHR$(2)                    :REM prompt for coordinate pair
1820 Z$=INPUT$(1,1)                     :REM trap echo'd character
1830 A$=INPUT$(1,1)                     :REM pen status byte
1840 B$=INPUT$(1,1)                     :REM X LS byte
1850 C$=INPUT$(1,1)                     :REM X MS byte
1860 D$=INPUT$(1,1)                     :REM Y LS byte
1870 E$=INPUT$(1,1)                     :REM Y MS byte
1880 Z$=INPUT$(1,1)                     :REM trap CR character
1890 IF ASC(A$)<>196 GOTO 1810          :REM pen not down , try again
1900 REM work out coord's XIN,YIN from these bytes...
1910 XIN=64*(ASC(C$)-128)+ASC(B$)-128
1920 YIN=64*(ASC(E$)-128)+ASC(D$)-128
1930 RETURN
1940 REM*************************************************************************
1950 REM new file , claer all arrays etc...
1960 REM*************************************************************************
1970 LC=0  :FOR N=0 TO 9
1980 NATTS(N)=0 :AVERR(N)=0
1990 FOR M=0 TO 21
2000 PERTN(N,M)=0
2010 NEXT M :NEXT N
2020 GOTO 560
2030 REM*************************************************************************
2040 REM error handling routine,traps i/o and file not found errors
2050 REM*************************************************************************
2060 IF ERR=57 THEN INPUT "dev.i/o.err,try again y/n";Y$:IF Y$= "Y" THEN RESUME
2070 IF ERR=53 THEN INPUT "file not found....OLD/NEW";Y$:IF Y$="OLD"THEN RESUME
2080 IF ERR=53 THEN RESUME 1970                          :REM file must be new
2090 IF ERR=71 THEN INPUT "disk not ready,again(y/n)";Y$:IF Y$= "Y" THEN RESUME
2100 PRINT "UNKNOWN ERROR...CODE=";ERR :ON ERROR GOTO 0 :CLOSE :END
2110 REM*************************************************************************
```

REFERENCES

1. SRS cavity microwave window failure investigations: preliminary problem analysis and literature review, Daresbury Lab. Tech. Memo DL/SCI/TM47A, (1986).

2. A. Wexler, Computation of electromagnetic fields, IEEE Trans. Microwave Theory Tech., 17, (1969) 416.

3. R. Mittra, Computer techniques for electromagnetics, (Germany: Pergamon Press, 1973).

4. J.B. Davies, Numerical solution of the hollow waveguide problem, Progress in Radio Science, 3, (1971) 307.

5. T. Tortschanoff, Survey of numerical methods in field calculations, Intermag Conf., Hamburg, 9-13 April, 1984 (invited paper).

6. A. Wexler, Solution of waveguide discontinuities by modal analysis, IEEE Trans. Microwave Theory Tech. 15, (1967) 508.

7. P.H. Masterman, Numerical solution of waveguide discontinuity problems, Ph.D. thesis, University of Leeds (1969).

8. S.W. Lee, W.R. Jones and J.J. Campbell, Convergence of numerical solutions of iris-type discontinuity problems, Proc. G-AP Int. Symp., Columbus, Ohio, 1970, pp.384-392.

9. P.H. Masterman, P.J.B. Clarricoats and C.D. Hannaford, Computer method of solving waveguide-iris problems, Electron. Lett., 5, (1969) 23.

10. P.S. Kooi, M.S. Leong and H. Thng, Application of modal analysis to a waveguide-cavity junction formed by an iris obstacle, Proc. IEE, 131, (1984) 35.

11. R.F. Harrington and J.R. Mautz, Characteristic modes for aperture problems, IEEE Trans. Microwave Theory Tech., 33, (1985) 500.

12. N. Perrone, Finite element and finite difference methods in engineering, Trans. ASME J. Mech. Des. (USA) 100, (1978) 188.

13. P.C. Jain and D.N. Holla, General finite difference approximation for the wave equation with variable coefficients using a cubic spline technique, Comput. Meths. Appl. Mech. Eng. 15, (1978) 175.

14. P.C.M. Lau, Numerical solution of Poisson's equation using curvilinear finite differences', Appl. Math. Modelling, (GB), 1, (1977) 349.

15. T.W. Edwards, Proton linear accelerator cavity calculations', M.U.R.A. report 622, 1961, (available from Office Tech. Serv., Dept. of Commerce, Washington D.C.)

16. R. Taylor and P. Kitching, Finite-difference computation of parameters of electromagnetic resonant cavities relevant to proton linear accelerators, NIRL/M/37, July 1962, Rutherford High Energy Lab., Harwell, Berks.

17. M. Albani and M. Bernardi, A numerical method based on the discretisation of Maxwell's equations in integral form, IEEE Trans. Microwave Theory Tech., 22, (1974) 446.

18. T. Weiland, Numerical solution of Maxwell's equations for static, resonant and transient problems, DESY, M-86-03 (April, 1986).

19. T. Weiland, On the unique numerical solution of Maxwellian eigenvalue problems in three dimensions' DESY, 84-111 (November 1984).

20. A. Sheffler, An overview of finite element methods and their application to engineering problems, RCA Review (USA), 39, (1978) 622.

21. O.C. Zienkiewicz, The Finite Element Method in Engineering Science, McGraw-Hill, London (1974).

22. J. Mathew and H.D. Brody, Analysis of heat transfer in continuous casting using a finite element method, Int. Conf. Comp. Sim. for Mats. Appl. Gaithersburg M.D., USA, 19-21 Apr. 1976, pt.II, pp.1138-50.

23. J. Mathew and H.D. Brody, Simulation of thermal stresses in continuous casting using a finite element method, ibid. pp.978-90.

24. A.F. Armor and M.K.V. Chari, Heat flow in the stator core of large turbine-generators by the method of three-dimensional finite elements, IEEE Trans. Power Appar. Syst., 5, (1976) 1648.

25. M.K.V. Chari, G. Bedrosian, J. Roeth and A. Konrad, Unification of electromagnetic and thermal analyses to determine losses and temperature distribution in a slot-embedded conductor, Proc. 8th U.F.E.M. Invitational Sym. Storrs CT, May 3, (Amsterdam: North-Holland, 1985), pp.61-81

26. A. Konrad, Electromagnetic devices and the application of computational techniques in their design, IEEE Trans. Magn., 21, (1985) 2382.

27. J. Simkin and C.W. Trowbridge, Electromagnetice CAD using a single user machine (SUM), IEEE Trans. Magn., 19, (1983) 2655.

28. D.A. Lowther, A microprocessor based electromagnetic field system, IEEE Trans. Magn., 18, (1982) 351.

29. A.D. McAulay, Variational finite element solution for dissipative waveguides and transportation application, IEEE Trans. Microwave Theory Tech., 25, (1977) 382.

30. P.P. Silvester, D.A. Lowther, C.J. Carpenter and E.A. Wyatt, Exterior finite elemsnts for 2-dimensional field problems with open boundaries, Proc. IEE, 124, (1977) 1267.

31. I. Babuska and W.C. Rheinboldt, On the reliability and optimality of the finite element method, Computers & Structures (GB), 10, (1979) 87.

32. Z.J. Csendes, Numerical solution of dielectric loaded waveguides: I. Finite elemsnt analysis, IEEE Trans. Microwave Theory Tech., 18, (1970) 1124.

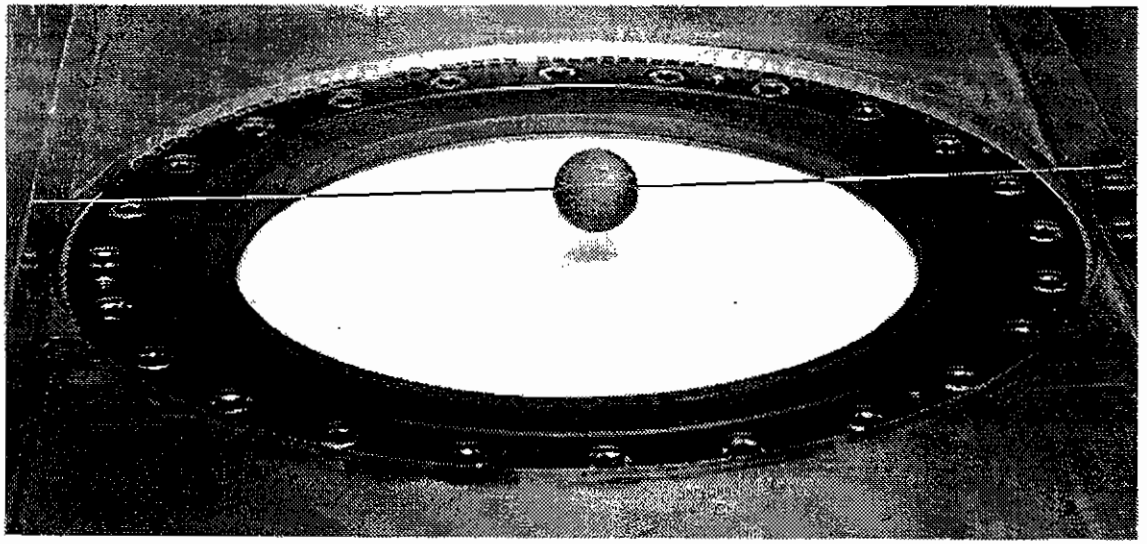

Fig.3

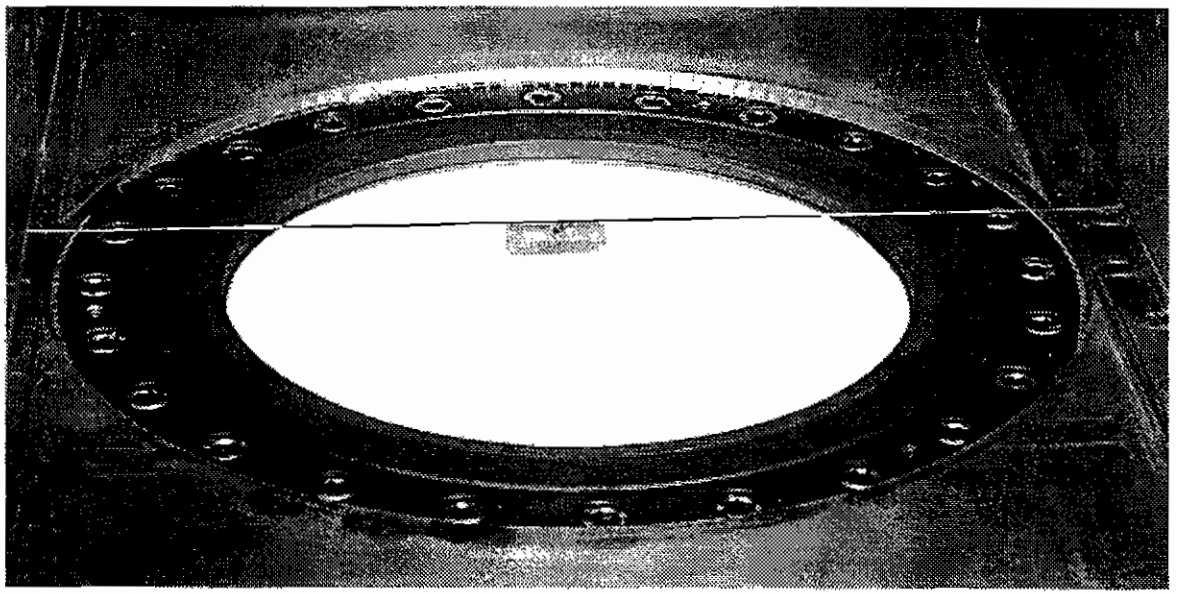

Fig.4

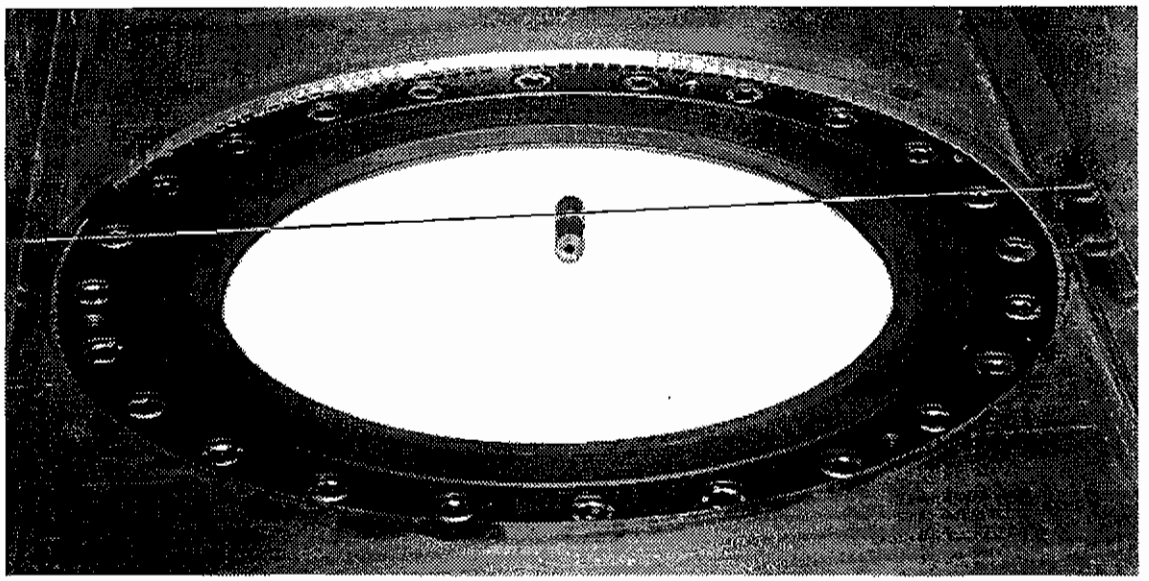

Fig.5

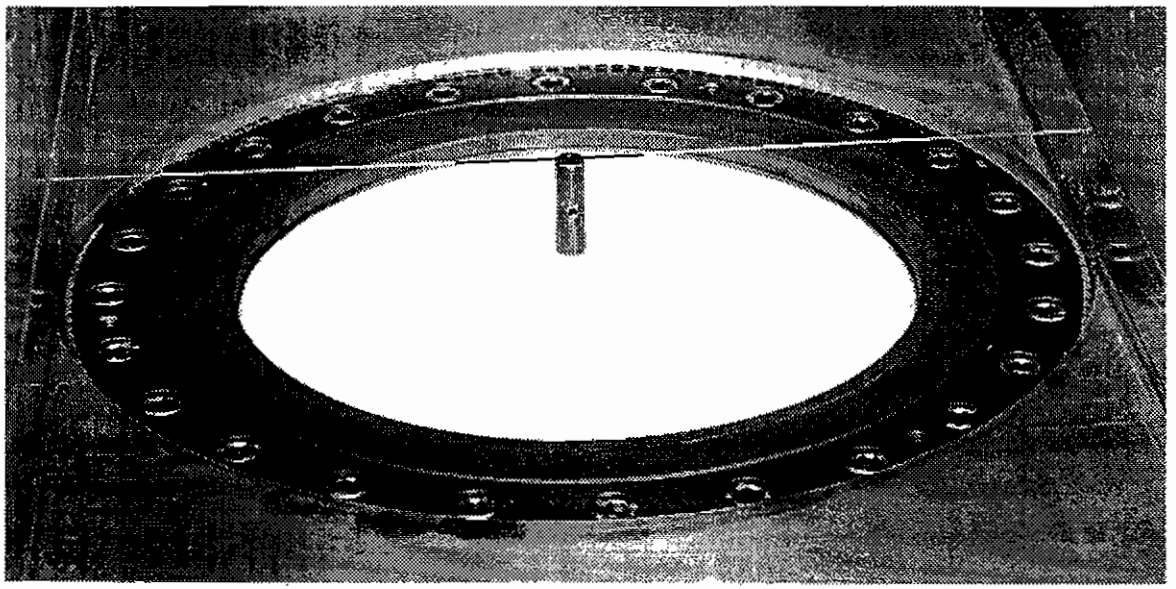

Fig.6

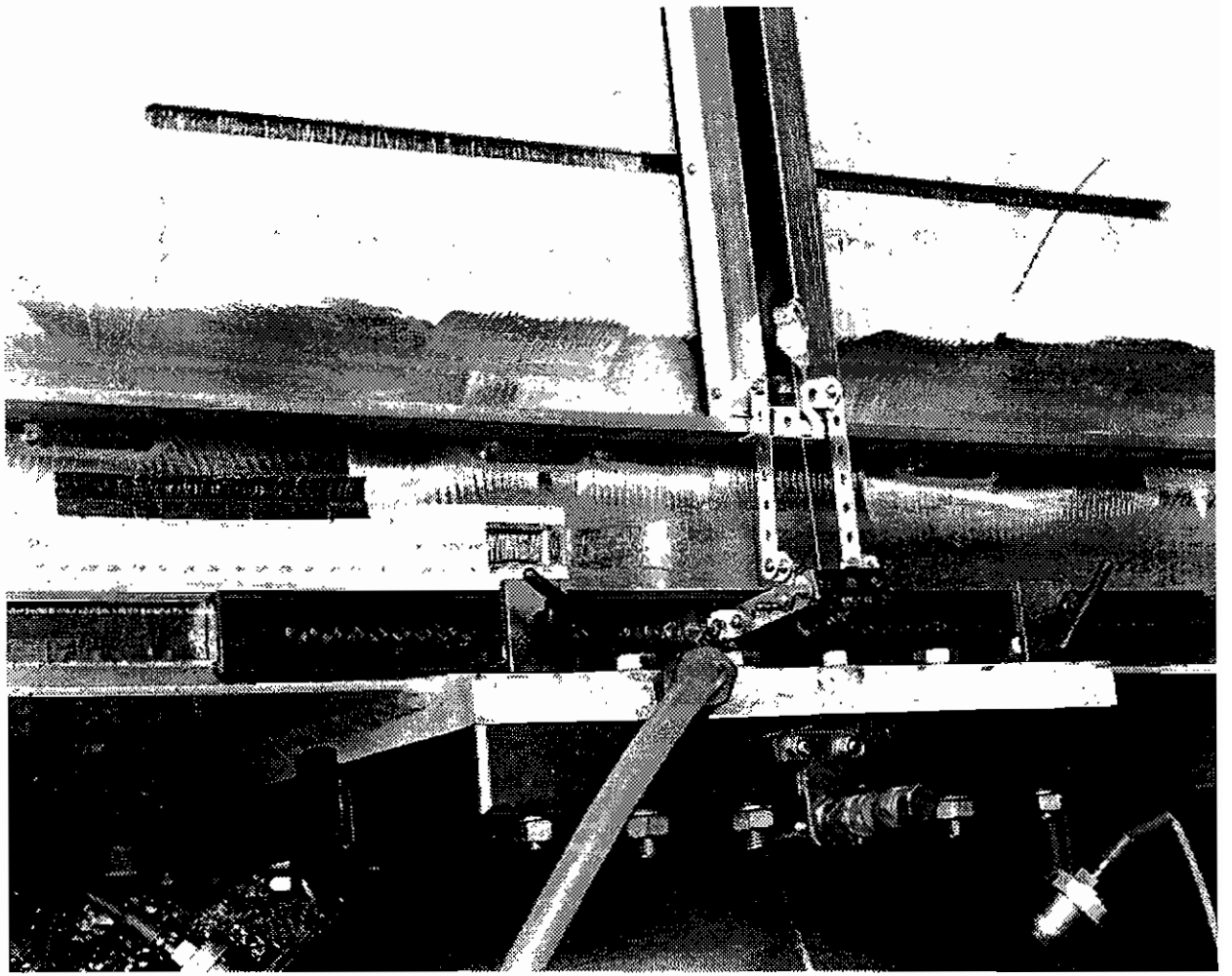

Fig.7

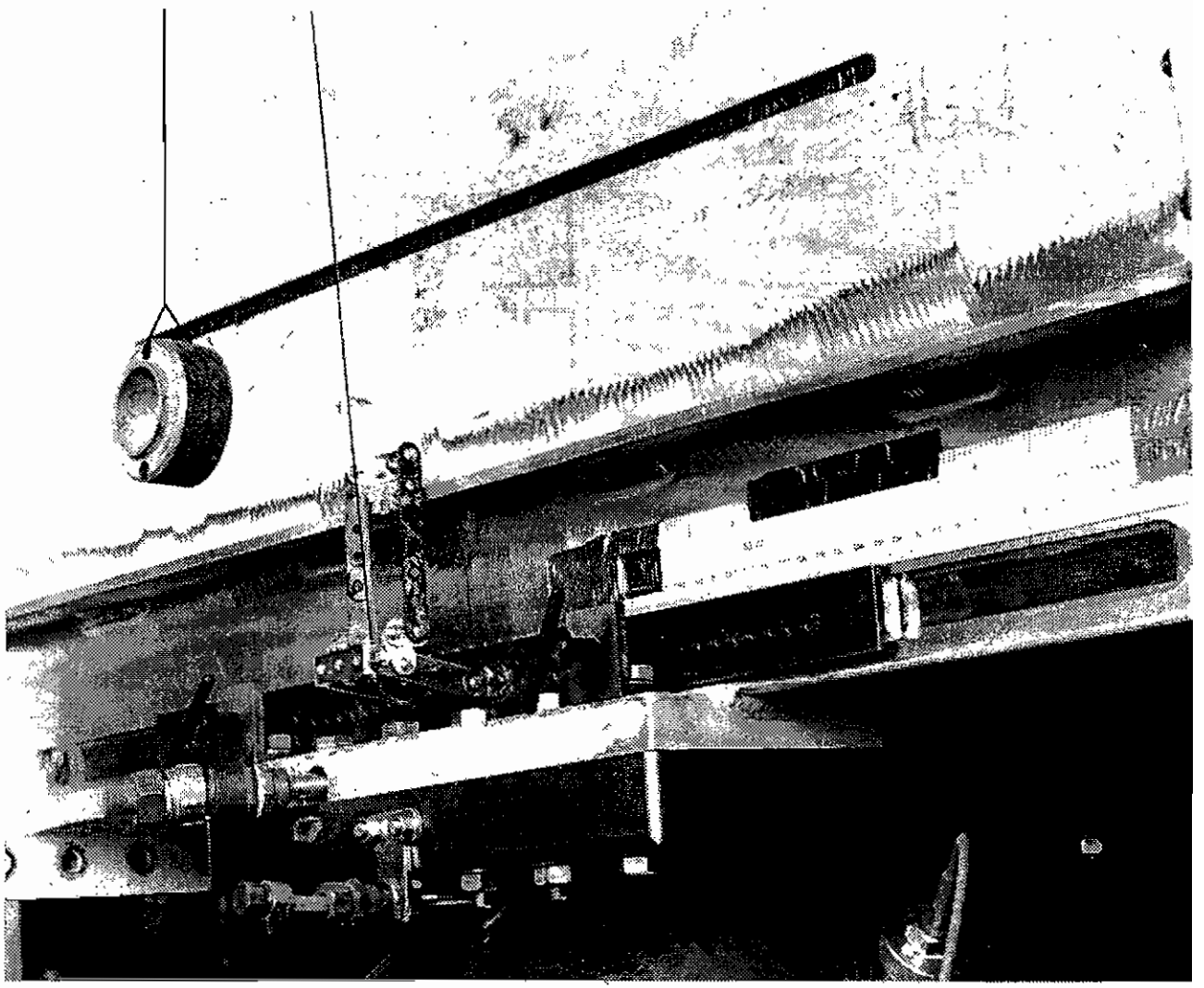

Fig.8

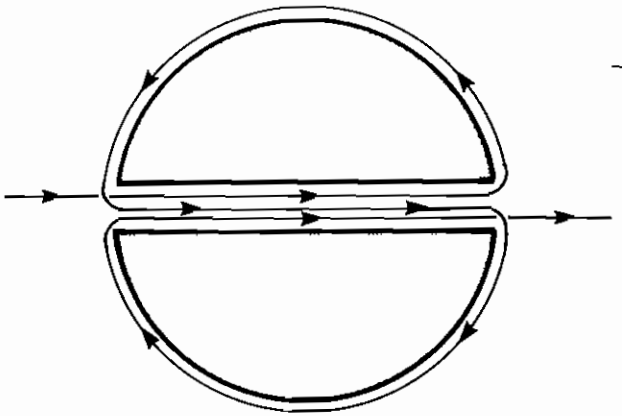

(a)
Bead *(threaded twice)*

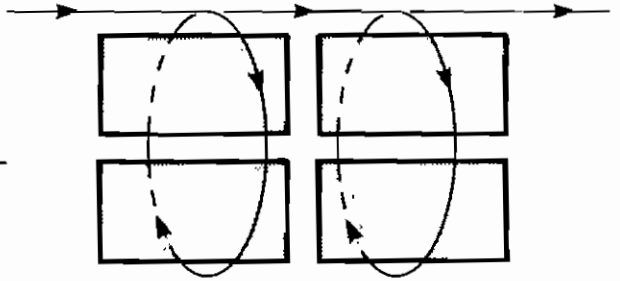

(b)
Rod slung below line *(x-orientation)*

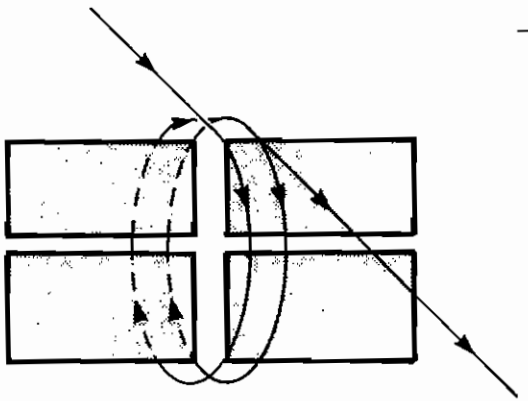

(c)
Rod *(y-orientation)*

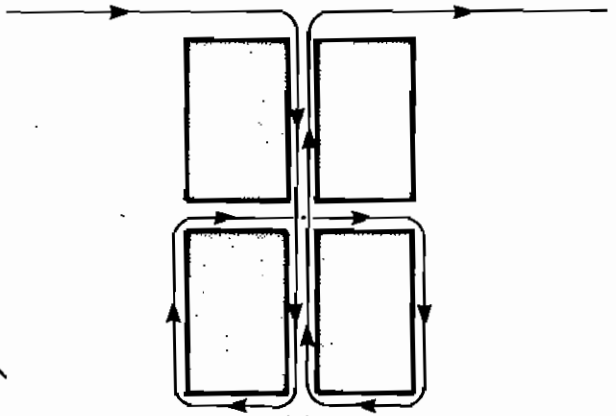

(d)
Rod vertical *(z-orientation)*

Fig.9

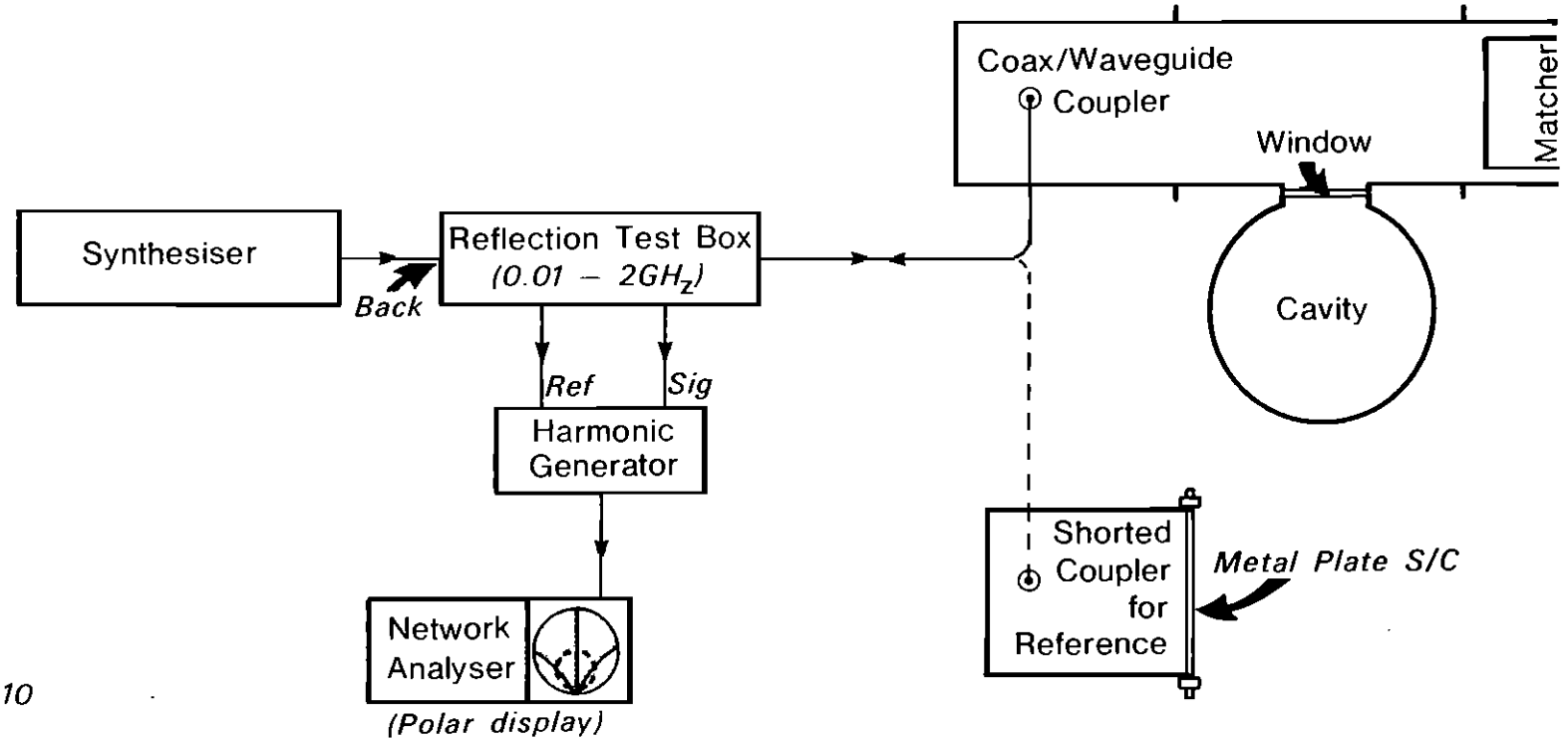
Coax/Waveguide
Coupler
Window
Matcher
Synthesiser
Reflection Test Box
(0.01 – 2GHz)
Back
Ref
Sig
Harmonic
Generator
Cavity
Shorted
Coupler
for
Reference
Metal Plate S/C
Network
Analyser
(Polar display)

Fig.10

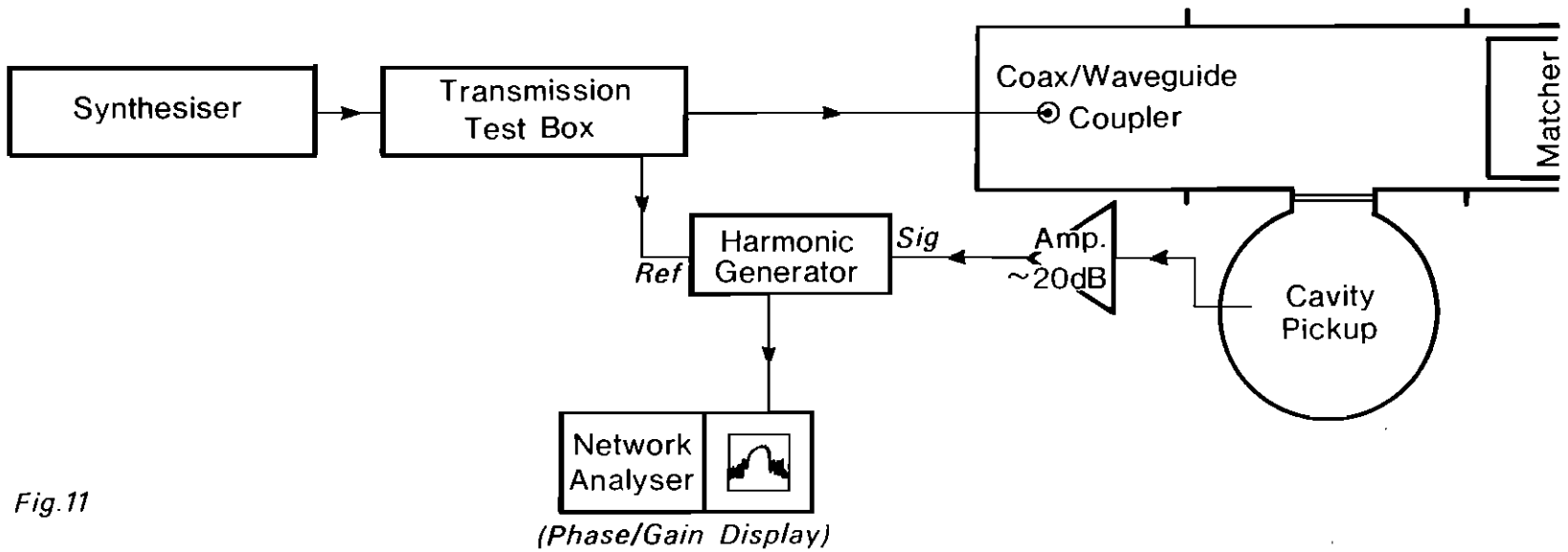
Synthesiser
Transmission
Test Box
Coax/Waveguide
Coupler
Matcher
Harmonic
Generator
Ref
Sig
Amp.
~20dB
Cavity
Pickup
Network
Analyser
(Phase/Gain Display)

Fig.11

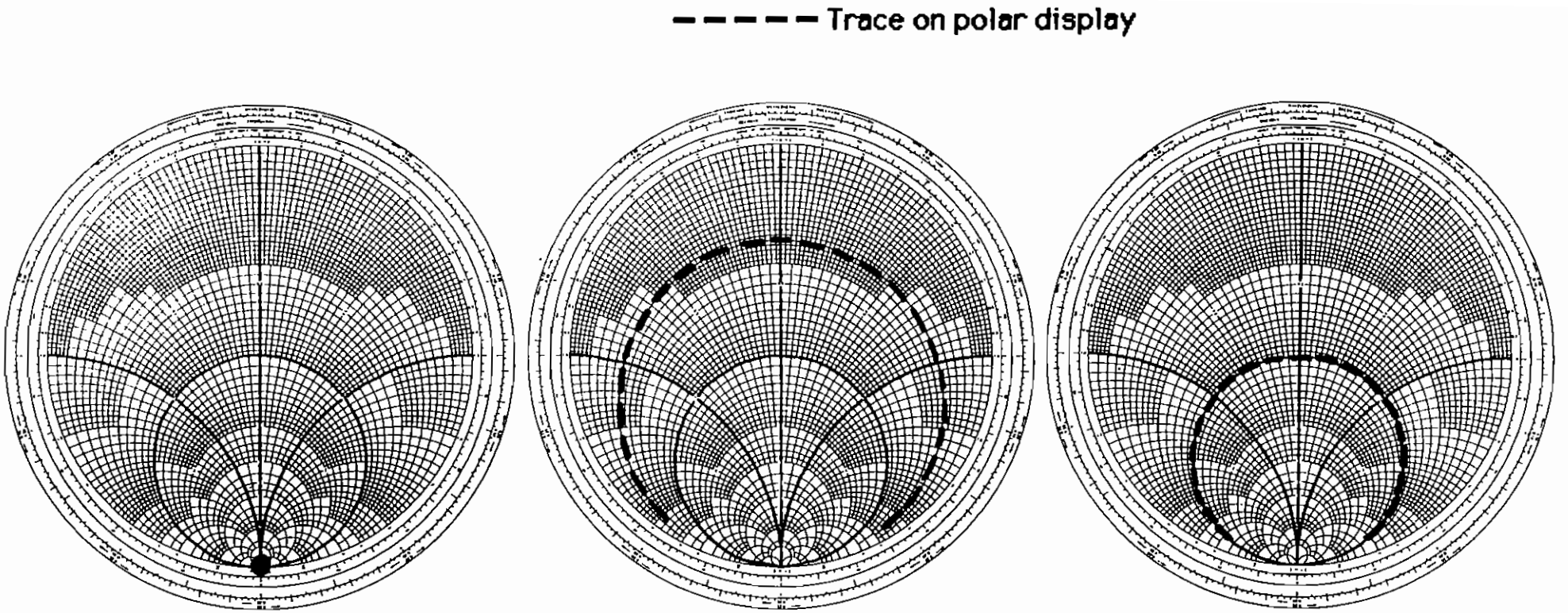
– – – – – Trace on polar display
(a) Spot on infinite VSWR position
(b) 300kHz sweep, poor match
(c) Good match, VSWR=1

Fig.12

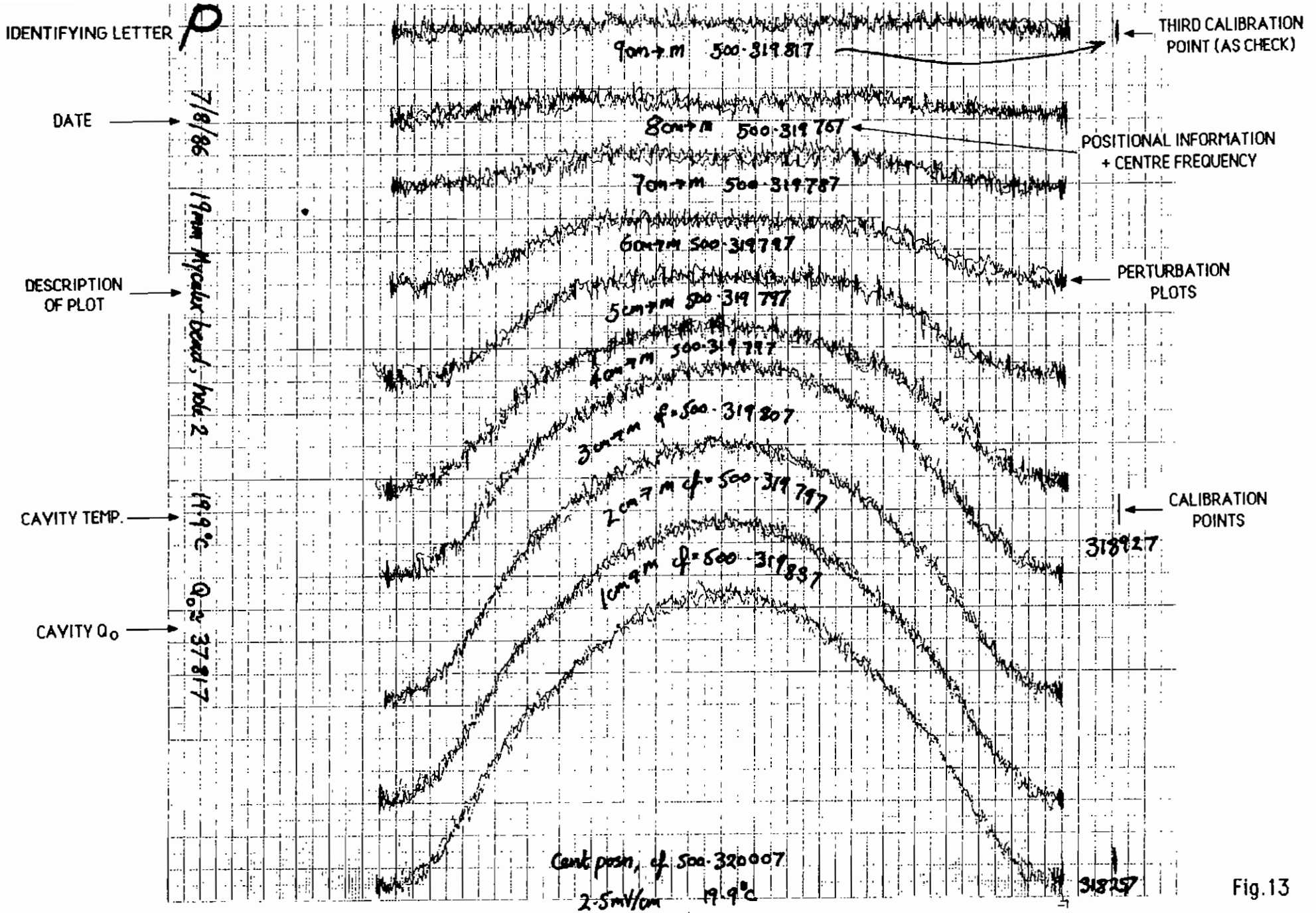
IDENTIFYING LETTER
DATE
DESCRIPTION OF PLOT
CAVITY TEMP.
CAVITY Q0
THIRD CALIBRATION POINT (AS CHECK)
POSITIONAL INFORMATION + CENTRE FREQUENCY
PERTURBATION PLOTS
CALIBRATION POINTS
9cm→m 500·319 817
8cm→m 500·319 767
7cm→m 500·319 787
6cm→m 500·319 797
5cm→m 500·319 797
4cm→m 500·319 787
3cm→m f=500·319 807
2cm→m f=500·319 797
1cm→m f=500·319 837
318927
318257
Cent posn, of 500·320007
2·5mV/cm 19·9°C

Fig.13

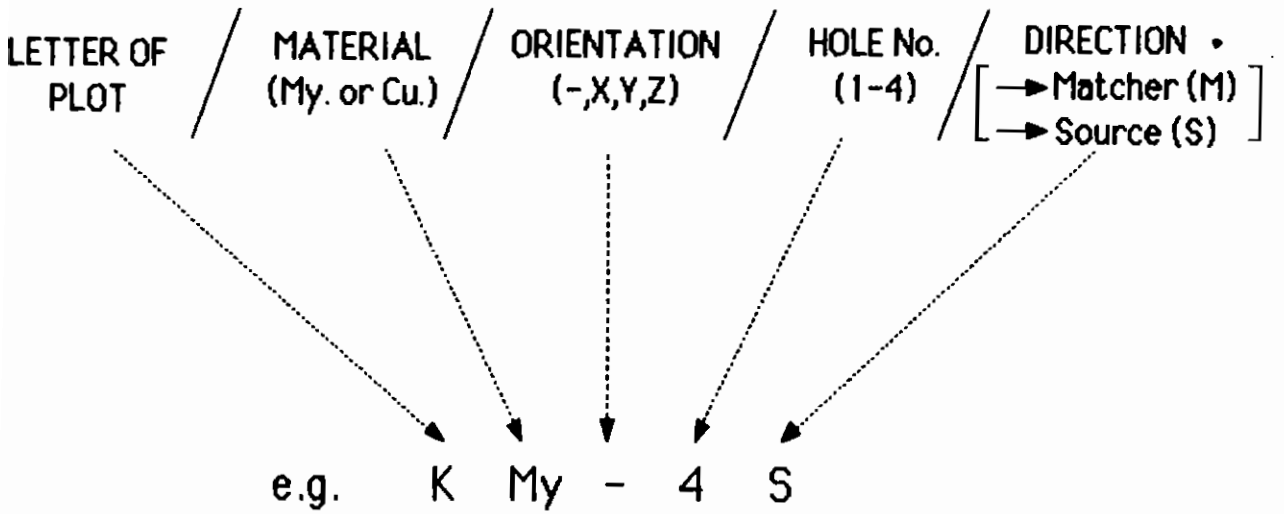
LETTER OF PLOT
MATERIAL (My. or Cu.)
ORIENTATION (-,X,Y,Z)
HOLE No. (1-4)
DIRECTION •
→Matcher (M)
→Source (S)
e.g. K My - 4 S

Fig.14

DATA FROM FILE PMy-2M

y\x	0	1	2	3	4	5	6	7	8	9	10	11	12	13	14	15	16	17	18	19	20	21 cm	
0 cm	-4	-15	-73	-174	-291	-349	-410	-458	-504	-525	-536	-535	-513	-482	-438	-386	-328	-261	-162	-60	-6	+0	av of 1 att's
1 cm	+1	-19	-83	-178	-274	-341	-397	-448	-486	-509	-513	-512	-498	-477	-437	-380	-328	-256	-167	-81	-18	+3	av of 1 att's
2 cm	+1	-19	-77	-160	-250	-323	-365	-400	-427	-448	-461	-459	-439	-417	-388	-346	-292	-231	-149	-61	-13	+6	av of 1 att's
3 cm	-4	-20	-56	-131	-210	-267	-299	-324	-355	-374	-383	-382	-377	-356	-332	-298	-251	-194	-124	-63	-16	+0	av of 1 att's
4 cm	-3	-13	-53	-99	-163	-216	-244	-264	-280	-292	-300	-296	-287	-267	-248	-222	-184	-137	-83	-23	-4	+3	av of 1 att's
5 cm	-4	-6	-25	-55	-109	-147	-172	-183	-188	-192	-188	-188	-184	-187	-179	-158	-133	-85	-47	-13	-3	+0	av of 1 att's
6 cm	+0	-5	-15	-40	-66	-91	-112	-120	-119	-119	-119	-121	-117	-113	-113	-102	-82	-64	-35	-20	-7	-2	av of 1 att's
7 cm	+1	-1	-4	-13	-27	-44	-54	-61	-61	-54	-50	-50	-55	-58	-58	-51	-34	-23	-12	+0	+3	+0	av of 1 att's
8 cm	-1	-7	-14	-17	-24	-33	-36	-35	-29	-25	-19	-19	-26	-27	-29	-33	-21	-13	-10	-3	-1	-1	av of 1 att's
9 cm	-4	-2	-7	-4	-8	-11	-12	-20	-18	-16	-14	-15	-13	-12	-13	-12	-15	-15	-12	-4	+0	+1	av of 1 att's

Fig. 15

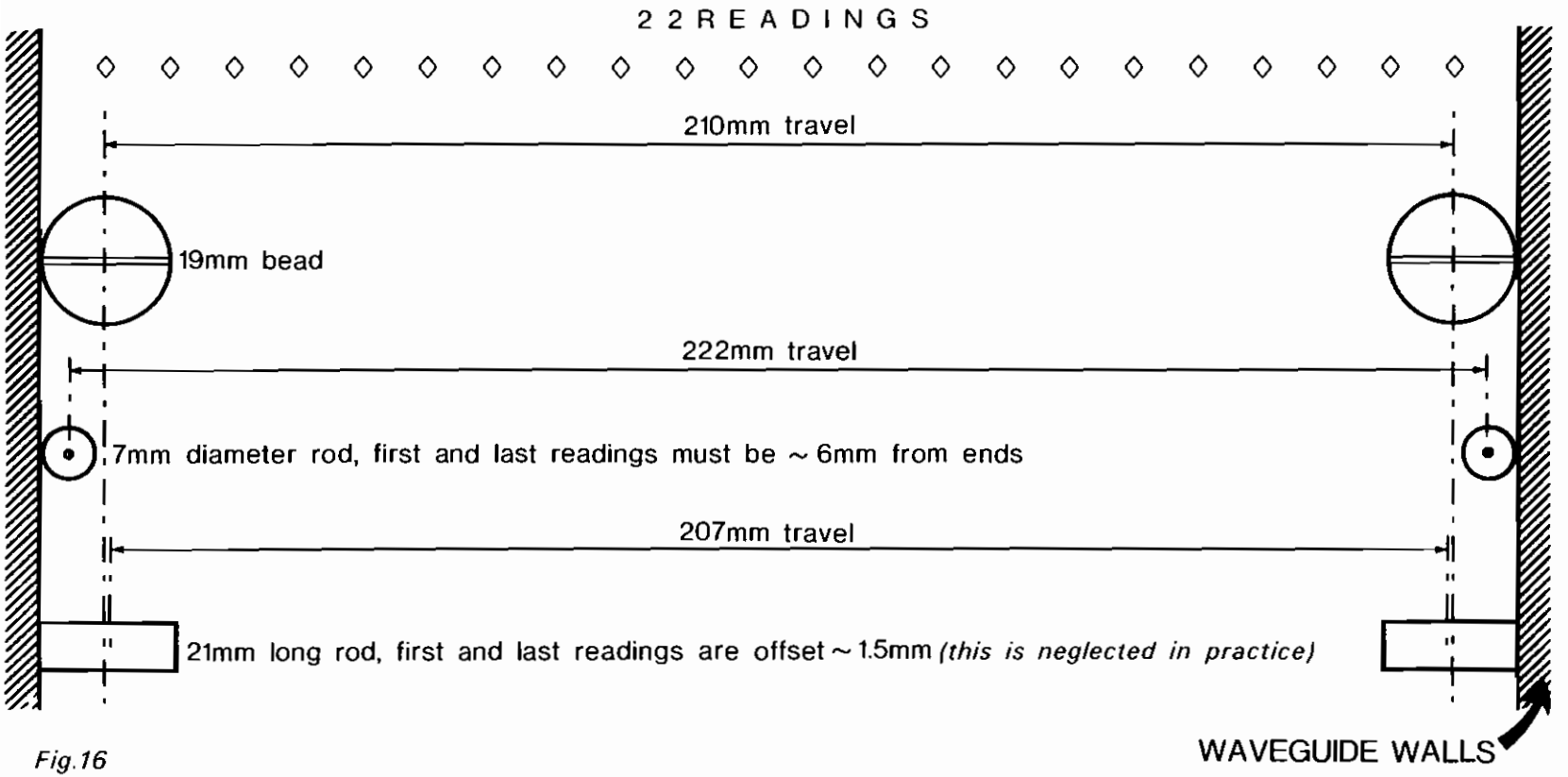
22 READINGS
210mm travel
19mm bead
222mm travel
7mm diameter rod, first and last readings must be ~ 6mm from ends
207mm travel
21mm long rod, first and last readings are offset ~ 1.5mm (this is neglected in practice)
WAVEGUIDE WALLS

Fig.16

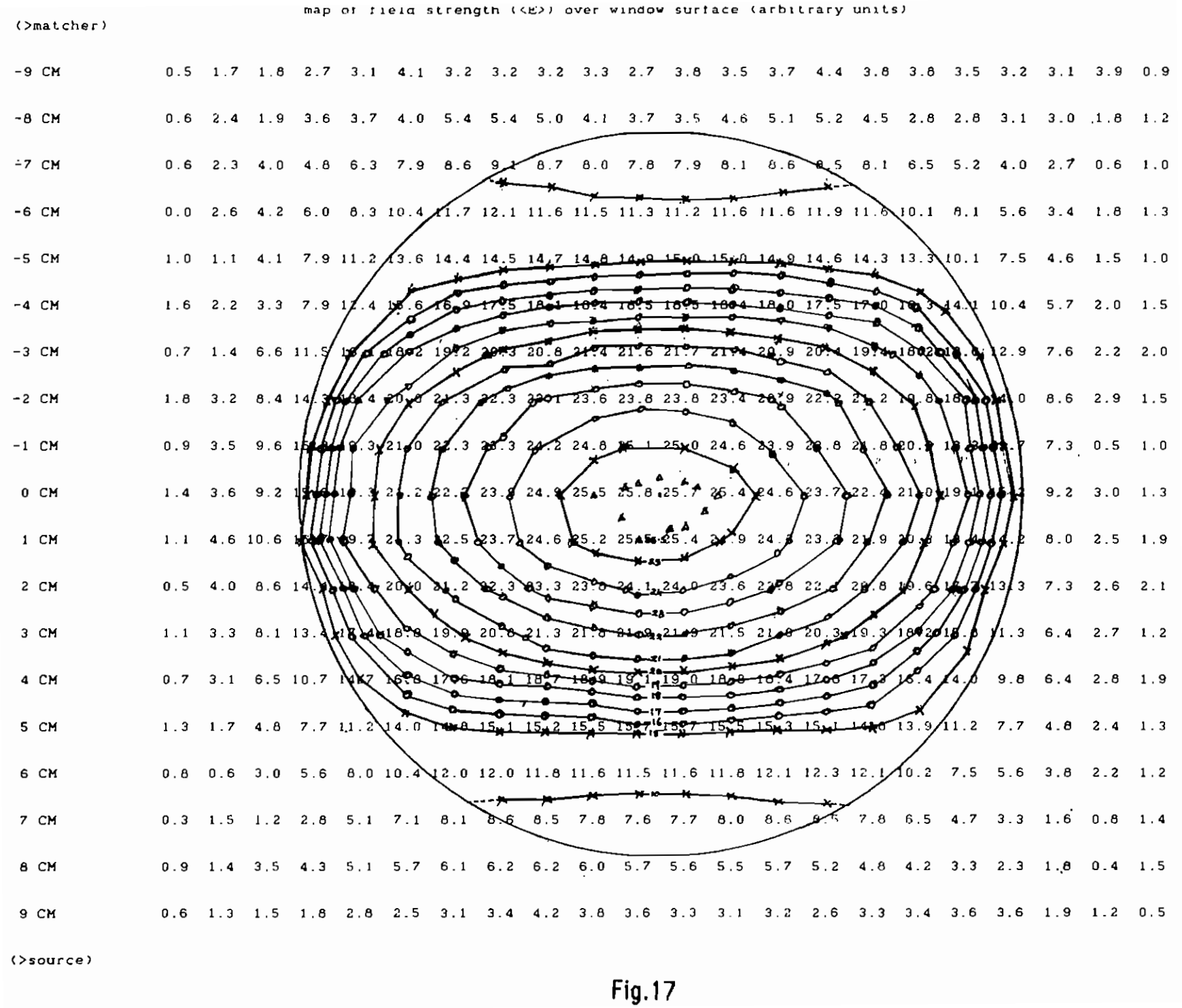
map of field strength (<E>) over window surface (arbitrary units)
(>matcher)
-9 CM 0.5 1.7 1.8 2.7 3.1 4.1 3.2 3.2 3.2 3.3 2.7 3.8 3.5 3.7 4.4 3.8 3.8 3.5 3.2 3.1 3.9 0.9
-8 CM 0.6 2.4 1.9 3.6 3.7 4.0 5.4 5.4 5.0 4.1 3.7 3.5 4.6 5.1 5.2 4.5 2.8 2.8 3.1 3.0 1.8 1.2
-7 CM 0.6 2.3 4.0 4.8 6.3 7.9 8.6 9.1 8.7 8.0 7.8 7.9 8.1 8.6 8.5 8.1 6.5 5.2 4.0 2.7 0.6 1.0
-6 CM 0.0 2.6 4.2 6.0 8.3 10.4 11.7 12.1 11.6 11.5 11.3 11.2 11.6 11.6 11.9 11.6 10.1 8.1 5.6 3.4 1.8 1.3
-5 CM 1.0 1.1 4.1 7.9 11.2 13.6 14.4 14.5 14.7 14.8 14.9 15.0 15.0 14.9 14.6 14.3 13.3 10.1 7.5 4.6 1.5 1.0
-4 CM 1.6 2.2 3.3 7.9 12.4 15.6 16.9 17.5 18.1 18.4 18.5 18.5 18.4 18.0 17.5 17.0 16.3 14.1 10.4 5.7 2.0 1.5
-3 CM 0.7 1.4 6.6 11.5 15.1 18.2 19.2 20.3 20.8 21.4 21.6 21.7 21.4 20.9 20.4 19.4 18.2 16.6 12.9 7.6 2.2 2.0
-2 CM 1.8 3.2 8.4 14.3 18.4 20.8 21.3 22.3 23.1 23.6 23.8 23.8 23.4 22.9 22.2 21.2 19.8 18.0 14.0 8.6 2.9 1.5
-1 CM 0.9 3.5 9.6 15.8 19.3 21.0 22.3 23.3 24.2 24.8 25.1 25.0 24.6 23.9 23.8 21.8 20.2 18.2 13.7 7.3 0.5 1.0
0 CM 1.4 3.6 9.2 15.8 19.3 21.2 22.5 23.8 24.9 25.5 25.8 25.7 25.4 24.6 23.7 22.4 21.0 19.1 14.2 9.2 3.0 1.3
1 CM 1.1 4.6 10.6 16.2 19.2 21.3 22.5 23.7 24.6 25.2 25.5 25.4 25.1 24.3 23.3 21.9 20.3 18.4 14.2 8.0 2.5 1.9
2 CM 0.5 4.0 8.6 14.7 18.4 20.0 21.2 22.3 23.3 23.9 24.1 24.0 23.6 22.8 22.1 20.8 19.6 17.7 13.3 7.3 2.6 2.1
3 CM 1.1 3.3 8.1 13.4 17.4 18.9 19.9 20.8 21.3 21.6 21.9 21.9 21.5 21.0 20.3 19.3 18.2 16.8 11.3 6.4 2.7 1.2
4 CM 0.7 3.1 6.5 10.7 14.7 16.8 17.6 18.1 18.7 18.9 19.1 19.0 18.8 18.4 17.8 17.3 16.4 14.0 9.8 6.4 2.8 1.9
5 CM 1.3 1.7 4.8 7.7 11.2 14.0 14.8 15.1 15.2 15.5 15.7 15.7 15.5 15.3 15.1 14.6 13.9 11.2 7.7 4.8 2.4 1.3
6 CM 0.8 0.6 3.0 5.6 8.0 10.4 12.0 12.0 11.8 11.6 11.5 11.6 11.8 12.1 12.3 12.1 10.2 7.5 5.6 3.8 2.2 1.2
7 CM 0.3 1.5 1.2 2.8 5.1 7.1 8.1 8.6 8.5 7.8 7.6 7.7 8.0 8.6 8.5 7.8 6.5 4.7 3.3 1.6 0.8 1.4
8 CM 0.9 1.4 3.5 4.3 5.1 5.7 6.1 6.2 6.2 6.0 5.7 5.6 5.5 5.7 5.2 4.8 4.2 3.3 2.3 1.8 0.4 1.5
9 CM 0.6 1.3 1.5 1.8 2.8 2.5 3.1 3.4 4.2 3.8 3.6 3.3 3.1 3.2 2.6 3.3 3.4 3.6 3.6 1.9 1.2 0.5
(>source)

Fig.17

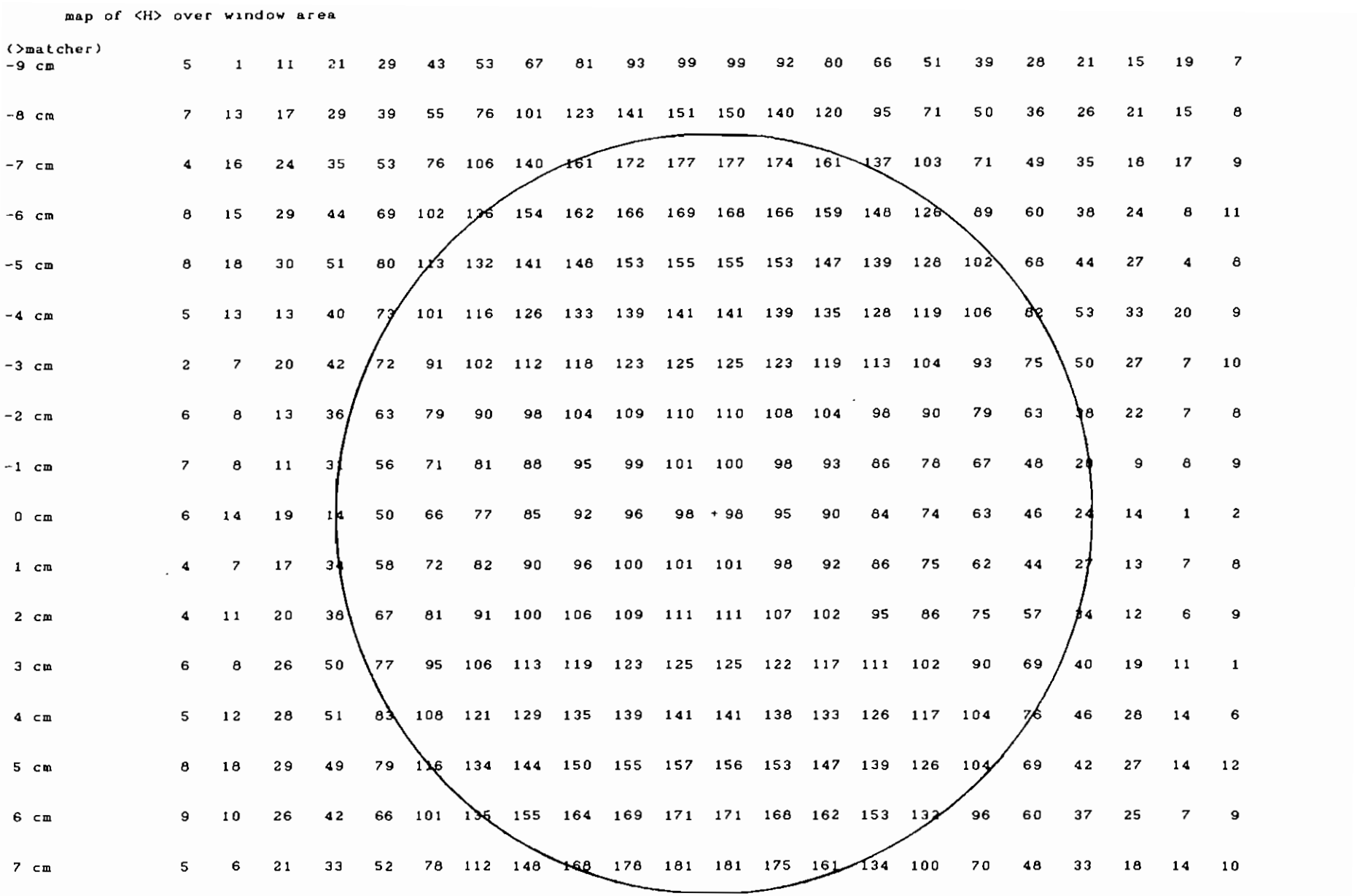

map of <H> over window area

(>matcher)

-9 cm	5	1	11	21	29	43	53	67	81	93	99	99	92	80	66	51	39	28	21	15	19	7
-8 cm	7	13	17	29	39	55	76	101	123	141	151	150	140	120	95	71	50	36	26	21	15	8
-7 cm	4	16	24	35	53	76	106	140	161	172	177	177	174	161	137	103	71	49	35	18	17	9
-6 cm	8	15	29	44	69	102	136	154	162	166	169	168	166	159	148	126	89	60	38	24	8	11
-5 cm	8	18	30	51	80	113	132	141	148	153	155	155	153	147	139	128	102	68	44	27	4	8
-4 cm	5	13	13	40	73	101	116	126	133	139	141	141	139	135	128	119	106	82	53	33	20	9
-3 cm	2	7	20	42	72	91	102	112	118	123	125	125	123	119	113	104	93	75	50	27	7	10
-2 cm	6	8	13	36	63	79	90	98	104	109	110	110	108	104	98	90	79	63	38	22	7	8
-1 cm	7	8	11	31	56	71	81	88	95	99	101	100	98	93	86	78	67	48	28	9	8	9
0 cm	6	14	19	14	50	66	77	85	92	96	98	+ 98	95	90	84	74	63	46	24	14	1	2
1 cm	4	7	17	34	58	72	82	90	96	100	101	101	98	92	86	75	62	44	27	13	7	8
2 cm	4	11	20	38	67	81	91	100	106	109	111	111	107	102	95	86	75	57	34	12	6	9
3 cm	6	8	26	50	77	95	106	113	119	123	125	125	122	117	111	102	90	69	40	19	11	1
4 cm	5	12	28	51	83	108	121	129	135	139	141	141	138	133	126	117	104	78	46	28	14	6
5 cm	8	18	29	49	79	116	134	144	150	155	157	156	153	147	139	126	104	69	42	27	14	12
6 cm	9	10	26	42	66	101	135	155	164	169	171	171	168	162	153	132	96	60	37	25	7	9
7 cm	5	6	21	33	52	78	112	148	168	178	181	181	175	161	134	100	70	48	33	18	14	10
8 cm	5	13	20	30	42	56	75	101	124	143	155	157	147	127	101	75	55	39	24	18	11	11
9 cm	3	11	15	20	32	42	54	69	83	95	100	100	94	81	64	51	42	30	25	16	10	7

(>source)

Fig.18

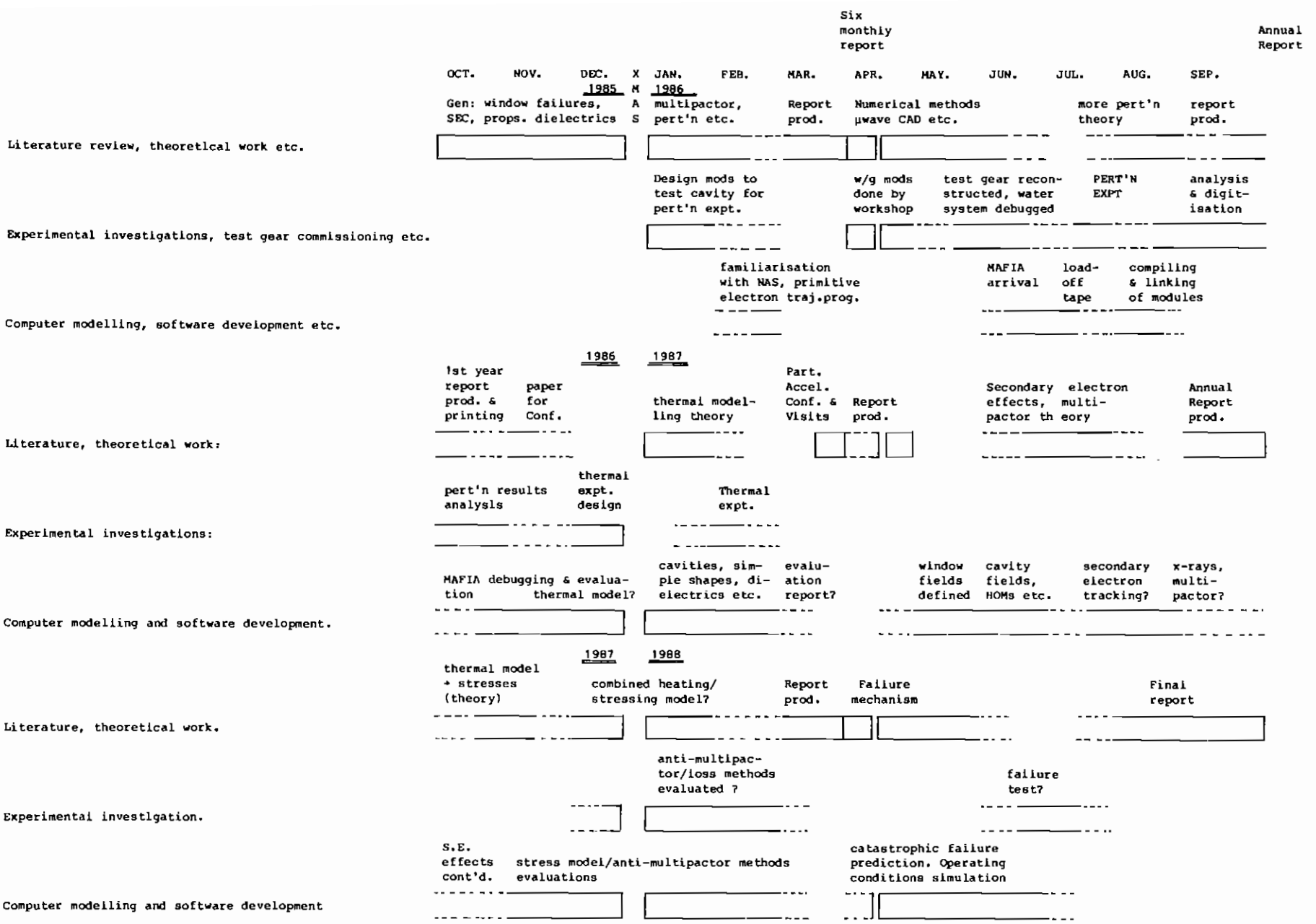

Fig.19. WINDOW FAILURE INVESTIGATION PROJECT PLAN (III) 9/86

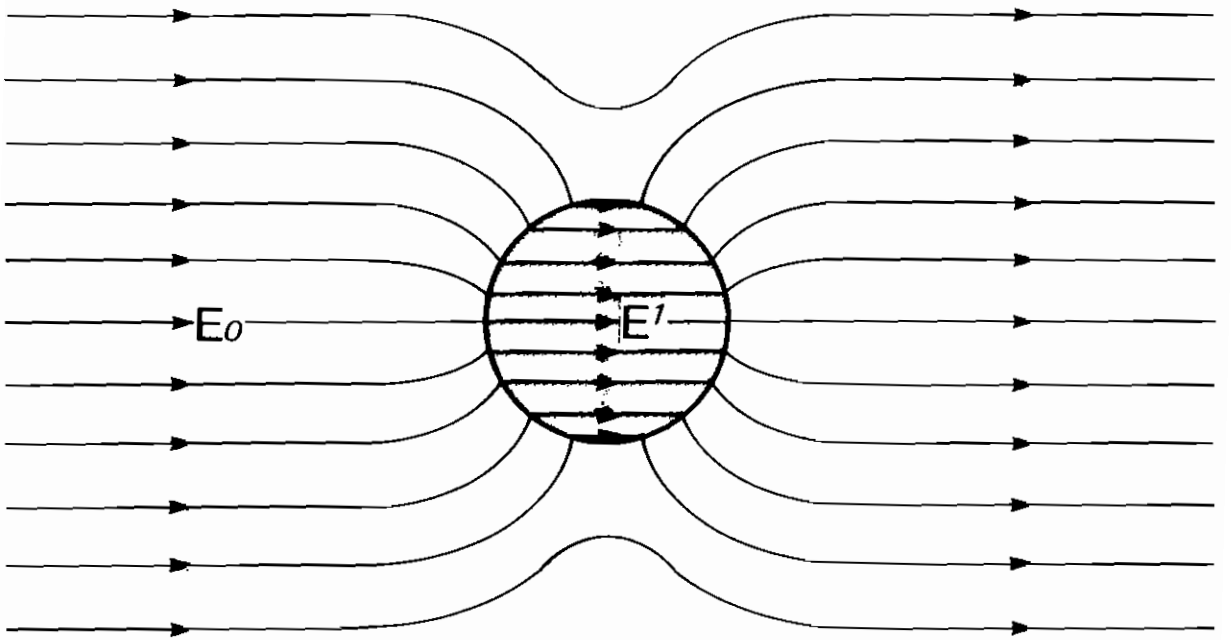

$$E^1 = \frac{3E_0}{\varepsilon_r + 2}$$

Fig. 20